Geophys. J. Int. (2008) **172,** 903–920 doi: 10.1111/j.1365-246X.2007.03653.x

Gravitational torque on the inner core and decadal polar motion

Mathieu Dumberry*

School of Earth and Environment, University of Leeds, Leeds LS2 9JT, *UK. E-mail:dumberry@ualberta.ca*

Accepted 2007 October 9. Received 2007 October 2; in original form 2007 April 16

SUMMARY

A decadal polar motion with an amplitude of approximately 25 milliarcsecs (mas) is observed over the last century, a motion known as the Markowitz wobble. The origin of this motion remains unknown. In this paper, we investigate the possibility that a time-dependent axial misalignment between the density structures of the inner core and mantle can explain this signal. The longitudinal displacement of the inner core density structure leads to a change in the global moment of inertia of the Earth. In addition, as a result of the density misalignment, a gravitational equatorial torque leads to a tilt of the oblate geometric figure of the inner core, causing a further change in the global moment of inertia. To conserve angular momentum, an adjustment of the rotation vector must occur, leading to a polar motion. We develop theoretical expressions for the change in the moment of inertia and the gravitational torque in terms of the angle of longitudinal misalignment and the density structure of the mantle. A model to compute the polar motion in response to time-dependent axial inner core rotations is also presented. We show that the polar motion produced by this mechanism can be polarized about a longitudinal axis and is expected to have decadal periodicities, two general characteristics of the Markowitz wobble. The amplitude of the polar motion depends primarily on the Y_2^1 spherical harmonic component of mantle density, on the longitudinal misalignment between the inner core and mantle, and on the bulk viscosity of the inner core. We establish constraints on the first two of these quantities from considerations of the axial component of this gravitational torque and from observed changes in length of day. These constraints suggest that the maximum polar motion from this mechanism is smaller than 1 mas, and too small to explain the Markowitz wobble.

Key words: Earth rotation variations; Dynamo: theories and simulations; Mantle processes; Elasticity and anelasticity.

1 INTRODUCTION

The rotation of the Earth, as observed from a reference frame fixed to the mantle, is nearly constant except for small variations in amplitude and direction. Changes in rotation rate are observable as changes in the length of day (LOD) whilst changes in the orientation of the rotation vector result in displacements of the rotation pole from the geographic North pole and are referred to as polar motion. Variations in LOD and polar motion occur on all observable timescales, from subdaily to millions of years. They are caused by external torques from the Moon, the Sun and other planets, by changes in the Earth's moment of inertia, and by exchanges of angular momentum between the mantle and the atmosphere, the oceans, and the fluid and solid cores. Though the variations are small, they contain a wealth of information about geophysical processes occurring at the surface or deep inside the Earth and they represent an indirect—and in some cases the only—observation of these processes.

The main sources of the variations in LOD and in polar motion at various timescales have been identified. However, a polar motion at decade timescales remains unexplained. This motion was first reported by Markowitz (Markowitz 1960, 1968), and is conventionally referred to as the Markowitz wobble in his honour. It was first described as a linear oscillation of the pole along the meridian 58°E with a period of 24 yr. Since then, it has been shown that the details of the decadal polar motion extracted from optical astrometry measurements prior to 1976 may not be very precise, but that the more reliable, higher precision space geodetic measurements after 1976 confirm nevertheless the existence of a decadal polar motion (Gross & Vondrák 1999; Vicente & Wilson 2002). While this motion is no longer considered to be periodic and along a fixed longitudinal plane, the mechanism that can generate a decadal polar motion with an amplitude of approximately 25 milliarcsecs (mas), or the more modest amplitude of 10 mas in the past 30 yr, remains unknown.

The more recent investigations of the role of surface processes in decade timescale polar motion have been conducted by using

*Now at: Department of Physics, University of Alberta, Edmonton, T6G 2G7 Canada.

climate models (Celaya *et al.* 1999; Ponte *et al.* 2002), atmosphere circulation models (de Viron *et al.* 2004), and data assimilation weather prediction models (Gross *et al.* 2005). The conclusion of all these studies is that surface processes cannot excite a polar motion of the amplitude and form of the Markowitz wobble. The polar motion resulting from an exchange of angular momentum between the core and the mantle by electromagnetic (Greff-Lefftz & Legros 1995) and topographic coupling (Greff-Lefftz & Legros 1995; Hide *et al.* 1996; Hulot *et al.* 1996) at the core–mantle boundary (CMB) is also incapable of explaining the Markowitz wobble.

Another possibility is that the Markowitz wobble may be a consequence of forced time-dependent changes in the orientation of the figure axis of the inner core. Because the angular momentum of the whole Earth has to be conserved, a tilt of the inner core results in an offset between the rotation axis and the figure axis of the mantle: a polar motion. This possibility was recently investigated by Greiner-Mai & Barthelmes (2001) and Dumberry & Bloxham (2002). This latter study showed that, in order to explain the amplitude of the signal, the required equatorial torque from surface forces on the inner core must be approximately 10^{20} N m. The same study suggested that a torque of this amplitude may be produced by electromagnetic coupling between the inner core and decadal azimuthal fluid motions called torsional oscillations. Moreover, the polar motion produced by this mechanism is polarized, as is the case for the Markowitz wobble. However, the estimate for the amplitude of the torque was based on a large axial differential rotation between torsional oscillations and the inner core. Because of the expected strong axial electromagnetic coupling at the inner core boundary (ICB), the inner core should be entrained to co-rotate with the mean zonal flows (Gubbins 1981). As a result, differential rotation between torsional oscillations and the inner core should be small. When this is taken into account the resulting equatorial electromagnetic torque is too small to explain the Markowitz wobble, a fact well illustrated by the study of Mound (2005).

In this paper, we investigate further the possibility that the rotational dynamics of the inner core may be responsible for the observed decadal polar motion. The scenario that we consider involves an inner core whose density structure at hydrostatic equilibrium is determined by the gravitational potential from density heterogeneities in the mantle. Because of electromagnetic coupling with torsional oscillations, we expect the inner core to be axially rotated out of its density alignment with the mantle. The longitudinal displacement of the non-axisymmetric density structure of the inner core produces a change in the moment of inertia of the whole Earth which, provided the density structure involves a spherical harmonic component Y_2^1, results in a polar motion. In addition, once the density structures of the inner core and the mantle are misaligned, a gravitational torque is established between the two. The axial component of this torque has been described by Buffett (1996a) and its effect on the variations in the LOD has been investigated by various authors (Buffett 1996b, 1998; Aurnou & Olson 2000; Mound & Buffett 2003, 2005, 2006). In this paper, we show that this gravitational torque also has an equatorial component. The latter leads to a tilt of the oblate geometric figure of the inner core with respect to the mantle. This produces a further change in the moment of inertia, and an additional polar motion which is larger and in the opposite direction to that which results from the axial rotation.

2 THE MARKOWITZ WOBBLE

In Fig. 1, we show the long period component of the polar motion since 1900. We have separated the signal in two different time-periods, 1900–1976 (Fig. 1a) and 1976–2007 (Fig. 1b). This is to illustrate the different character of the decadal period polar motion captured by classical astrometry until 1976 and that derived from space geodetic techniques from 1976 onward. The curve shown on Fig. 1(a) was obtained by applying a third order low-pass Butterworth filter with a cut-off period of 10 yr to the polar motion time-series POLE2005 which covers the period 1900–2005 (Richard S. Gross, personal communication, 2006). A linear trend of 1.10 mas yr^{-1} in the direction m_1 and -3.26 mas yr^{-1} in the direction m_2 has been removed. Time-series POLE2005 consists of data from the International Latitude Service (ILS) until 1962, data

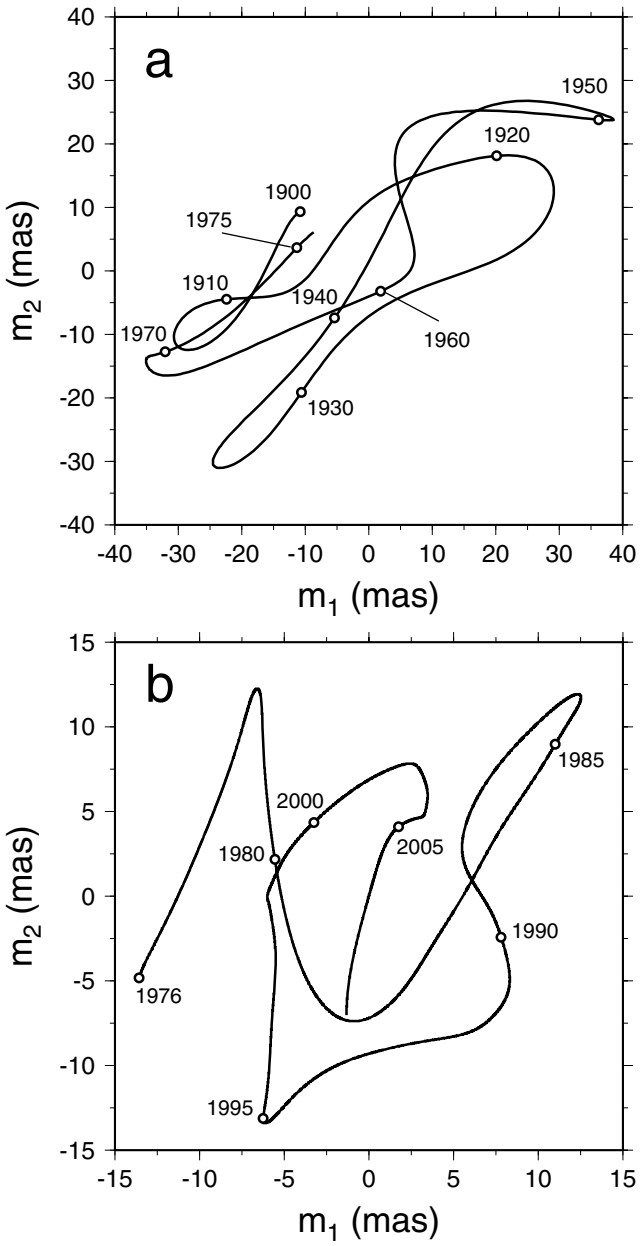

Figure 1. The trajectory of the mean position of the rotation axis with respect to a fixed point at the surface for the time-periods (a) 1900–1976 (from time-series POLE2005) and (b) 1976–2007 (from time-series EOP-C04). The direction m_1 is aligned with the Greenwich meridian. As an indication of the amplitude of the motion, 30 mas corresponds approximately to 1 m. For each time-period, a linear trend has been removed and higher frequency signals have been filtered. The location of the origin is arbitrary.

coming from a wider variety of astrometric observations between 1962 and 1976, and space-geodetic data from 1976 onward. The description of an earlier version of this time-series can be found in Gross (2000). More thorough data analyses have been performed on this time-series, and others, in order to isolate the decadal polar motion (e.g. Vicente & Wilson 2002), though our simple low-pass filter is sufficient to capture the salient features of the signal (compare Fig. 1a with fig. 6 of Vicente & Wilson (2002)). The curve shown in Fig. 1(a) represents the motion that is usually referred to as the Markowitz wobble, a quasi-periodic signal with a period of approximately 30 yr, an amplitude of approximately 25 mas, and generally polarized in a longitudinal axis close to 45°E (e.g. Vicente & Currie 1976; Wilson & Vicente 1980; Dickman 1981; Poma *et al.* 1987). The signal in Fig. 1(b) shows the decadal polar motion captured by space-geodetic technique since 1976. This curve was obtained by applying a third order low-pass Butterworth filter with a cut-off period of 5 yr to the polar motion time-series EOP-C04 of the International Earth Rotation Service (IERS) between 1976 and 2007. A linear trend of 0.90 mas yr^{-1} in the direction m_1 and -3.02 mas yr^{-1} in the direction m_2 has been removed. In contrast to the signal before 1976, the decade polar motion in Fig. 1(b) is of smaller amplitude (approximately 10 mas), does not appear to have a specific periodicity, nor a preferred orientation.

The very existence of the Markowitz wobble of Fig. 1(a) was once a matter of debate, as there was a worry that the signal may be an artefact from a change in star catalogue (e.g. Munk & MacDonald 1960; Lambeck 1980). This concern has since been dismissed, as it was shown that the signal remained once the appropriate corrections were made (Vondrák 1999). In addition, decadal variations are clearly present in the space geodetic time-series as shown in Fig. 1(b), providing further confirmation for the existence of long period polar motions. However, the general character of the more reliable signal in the past 30 yr is different than that captured by astrometric techniques prior to 1976. This suggests that, although we expect a decadal polar motion to have been present before 1976, the details of the optical-era signal in Fig. 1(a) may not be entirely reliable. Indeed, it has been shown that, during their period of overlap between 1976 and 1992, the decadal period polar motion derived from optical and space geodetic techniques are poorly correlated (Gross & Vondrák 1999; Vicente & Wilson 2002). Hence, the polarisation and the periodicity of the signal in Fig. 1(a) may not be robust, and its amplitude of 25 mas may be exaggerated. Although the decadal polar motion may still be referred to as the Markowitz wobble, as we do in this study, it is generally no longer considered to be strictly periodic nor oriented along a fixed longitudinal plane.

The origin of the decadal polar motions shown in Fig. 1 remains a mystery. No mechanism has been shown capable of producing a signal with an amplitude of least 10 mas on a decadal timescale. Although one must consider the pre-1976 decadal signal with caution, explaining the larger amplitude and polarisation of the signal shown in Fig. 1(a) represents an even greater challenge. The point of view that we adopt in this study is to consider the problem from the perspective of the dynamics. If a mechanism can be shown to produce a polar motion with similar characteristics as that of Fig. 1(a), it will tend to support the existence of such a signal, and also provide an explanation for it. Since the details of the decadal polar motion may not be well constrained in the optical era, the object is not try to reproduce the exact features of the curve shown in Fig. 1(a), but only its general characteristics. We thus seek a mechanism that can produce a decadal timescale polar motion which is polarized, and with an amplitude of approximately 25 mas. If we restrict our goal to explaining only the signal after 1976, then a smaller polar motion with an amplitude of 10 mas must be achieved, and polarisation is no longer a required feature of the signal.

3 GRAVITATIONAL TORQUE ON THE INNER CORE

3.1 Density structure

The density structure inside the Earth is determined by a balance of force between gravity, centrifugal acceleration and surface forces. If the Earth were not rotating nor convecting, the surfaces of constant density ρ would be spherically symmetric, with density increasing towards the centre. The centrifugal acceleration from Earth's rotation deforms the surfaces of constant density into an elliptical shape. The ellipticity is small, as gravity remains much larger than the centrifugal force, but it is the largest of the non-spherical density features. The slightly oblate surfaces of constant density coincide with equipotential surfaces (i.e. the sum of gravitational and centrifugal potential) and define a basic hydrostatic reference state.

In the mantle, smaller density variations about this hydrostatic equilibrium arise from the mass anomalies involved in convective motions. These also include the contribution from topography at density discontinuities such as at the Earth's surface and the CMB. Convection occurs in the fluid core as well, but the scale of the mass anomalies involved, $\delta\rho/\rho \sim 10^{-8}$ (Stevenson 1987), is much smaller than those in the mantle. As a result, the largest perturbation to the oblate reference density structure in the fluid core is not due to its own convective dynamics, but is controlled instead by the distribution of density heterogeneities in the mantle. This is because the fluid core must preserve its hydrostatic equilibrium, and so its surfaces of constant density must deform to coincide with the gravitational potential associated with the mantle density heterogeneities. The amplitude in the density perturbation from this effect is of the order of $\delta\rho/\rho \sim 10^{-4}$ (Buffett 1996a), much larger than the density anomalies involved in core convection. Inside the inner core, if we assume that no convection takes place, the leading density heterogeneities are also controlled by the convective mass anomalies of the mantle. This is provided the inner core's viscosity is smaller than that of the mantle. If it is the case, over timescales longer than its viscous relaxation time, the inner core can be considered a hydrostatic fluid, and the physical picture used to describe the fluid core also applies to the inner core. The mass anomalies in the mantle, therefore, produces an imprint on the density structure of the whole of the core.

Mathematically, we may express the density structure everywhere inside the Earth in terms of a spherical harmonic expansion

$$\rho(\mathbf{r}) = \rho_{\rm o} + \rho_\epsilon Y_2^0 + \sum_{l,m} \rho_l^m Y_l^m, \tag{1}$$

where

$$\sum_{l,m} = \sum_{l=1}^{\infty} \sum_{m=-l}^{l}. \tag{2}$$

In this definition, the position vector $\mathbf{r}$ points from the origin to the point (r, θ, ϕ) in spherical coordinates, and $\rho_{\rm o} = \rho_{\rm o}(r)$ and $\rho_\epsilon = \rho_\epsilon(r)$ are, respectively, the spherically symmetric and elliptical components of the density distribution that defines the reference hydrostatic state. The coefficients $\rho_l^m = \rho_l^m(r)$ represent the amplitude of the density heterogeneity due to mantle mass anomalies (or its imprint in the core) at spherical harmonic degree l and order m, and $Y_l^m = Y_l^m(\theta, \phi)$ are fully normalized spherical harmonic

functions, i.e.

$$\int_{\Omega} Y_l^{m*} Y_{l'}^{m'} \, \mathrm{d}\Omega = \delta_{ll'} \delta_{mm'}. \tag{3}$$

For arguments stated above, $\rho_l^m < \rho_\epsilon \ll \rho_\mathrm{o}$.

An alternative representation of the density structure, one which is more convenient for subsequent manipulation, is to define instead the surfaces on which the density ρ_o is uniform (Jeffreys 1970),

$$r = a \left(1 + \epsilon Y_2^0 + \sum_{l,m} \varepsilon_l^m Y_l^m \right), \tag{4}$$

where a is the mean spherical radius, $\epsilon = \epsilon(a)$ is the amplitude of the elliptical flattening, and $\varepsilon_l^m = \varepsilon_l^m(a)$ is the amplitude of the equivalent density deformation due to mantle mass anomalies at degree l and order m. Under this representation, the density is now only function of a: $\rho_\mathrm{o} = \rho_\mathrm{o}(a)$. As was the case above, we expect $\varepsilon_l^m < \epsilon \ll 1$.

3.2 Simple description of the angular momentum balance and gravitational torque

The manner in which the rotational dynamics of the inner core influences the orientation of the Earth's rotation vector can be understood from simple considerations of angular momentum. A tilt of the elliptical figure of the inner core in an equatorial direction results in a change in the moment of inertia and, as a consequence, also a change in angular momentum. For the Earth to conserve its own angular momentum, an equal but opposite change in angular momentum must take place in the mantle and fluid core. This is achieved by a reverse equatorial rotation of their combined body about the Earth's rotation axis (which coincides with the angular momentum vector). Thus, as illustrated in Fig. 2, from a mantle's perspective, a tilt of the inner core is accompanied by an offset of the Earth's rotation axis: a polar motion. More generally, any internal density reorganisation affecting the spherical harmonic component Y_2^1, such as a tilt of the elliptical inner core, induces a polar motion (e.g. Lambeck 1980).

In this paper, we investigate whether the observed decadal polar motion can be due to the rotational dynamics of the inner core. The

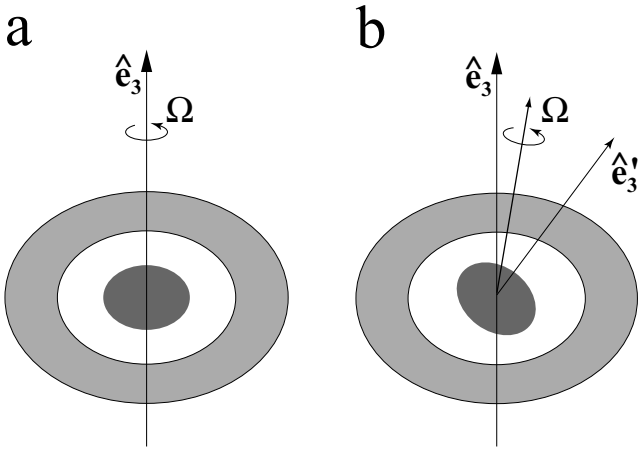

Figure 2. (a) The equilibrium configuration of the Earth where the elliptical mantle (light grey), fluid core (white) and solid inner core (dark grey) are all aligned and rotating at angular velocity $\mathbf{\Omega}$. (b) The equilibrium configuration when the inner core is tilted, based on conservation of angular momentum. $\hat{\boldsymbol{e}}_3$ and $\hat{\boldsymbol{e}}_3'$ are the axes of geometric symmetry of the oblate figures of the mantle and inner core, respectively. Not drawn to scale.

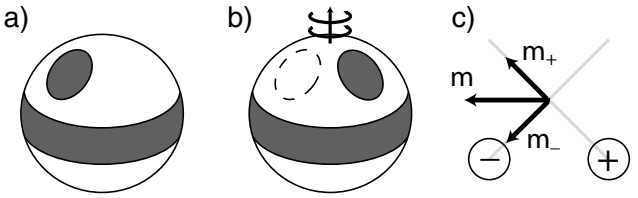

Figure 3. (a) The non-spherical density of the inner core comprised of an elliptical component (depicted by an equatorial band) and a mid-latitude non-axisymmetric positive anomaly (the oval shape) which includes a Y_2^1 component; (b) The density structure of the inner core, as viewed from the mantle, after an axial rotation; (c) Viewed in the equatorial plane, the axial rotation of the inner core creates a mass deficit (−) and a mass surplus (+), thereby changing the moment of inertia. The polar motion in response includes a component directed away from the mass surplus (m_+) and one towards the mass deficit (m_-): the resulting polar motion is directed along the vector m.

scenario that we envisage involves a time-dependent axial rotation of an inner core that has a non-axisymmetric density structure. As illustrated in Fig. 3, such a rotation leads to a change in the internal Y_2^1 density component and to a polar motion. The direction of the polar motion is such that the excess mass is moved towards the equator. Once the density structure of the inner core is longitudinally misaligned with respect to that of the mantle, an equatorial gravitational torque is set up between the two. This leads to a tilt of the elliptical inner core with respect to the mantle, and to a further polar motion.

Why an equatorial gravitational torque occurs is most easily visualized with the help of simple illustrations. Suppose that, as shown in Fig. 4(a), the aspherical density structure in the mantle is comprised of an elliptical component ρ_ϵ—the result of Earth's rotation—and a non-axisymmetric positive mass anomaly at mid-latitude. The equilibrium density structure of the inner core is also comprised of a rotationally induced elliptical component and a mid-latitude positive mass anomaly from the imposed gravitational potential of the mantle (Fig. 4b). In this equilibrium configuration, there is no net torque on the inner core. The gravitational force on the equatorial axisymmetric part of the inner core density (AIC) due to its interaction with the equatorial axisymmetric density of the mantle (AM) has no lateral component, and neither does the gravitational force on the non-axisymmetric part of the inner core density (NAIC) due to the non-axisymmetric density of the mantle (NAM). The gravitational force on the NAIC from its interaction with the AM does have a lateral component and an associated torque (Γ_1 on Fig. 4d), but this torque is exactly balanced by that due to the gravitational force of the NAM on the AIC (Γ_2 on Fig. 4e), so there is no net torque (Fig. 4f).

An axial rotation of the inner core with respect to a fixed mantle perturbs this equilibrium. The AIC is unaffected by an axial rotation, but the NAIC is longitudinally displaced (Fig. 4c). The gravitational interaction between the NAIC and the NAM results in an azimuthal force, or an axial torque, that acts to restore the alignment. This axial gravitational torque was identified first by Buffett (1996a). This misalignment also lead to a torque in the equatorial direction. As shown in Fig. 4(h), the torque Γ_2 from the interaction between AIC and NAM is unaffected by an axial rotation. However, as NAIC is axially rotated, so is the torque Γ_1 from its interaction with AM (Fig. 4g). As a result, Γ_1 and Γ_2 no longer cancel one another and their sum produce a net equatorial torque on the inner core (Fig. 4i).

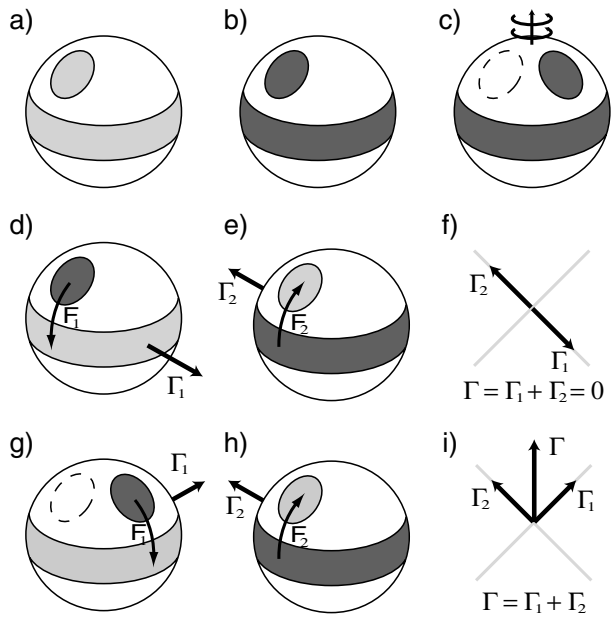

Figure 4. (a) The non-spherical density of the mantle (light grey) comprised of an elliptical component (depicted by an equatorial band and referred to as AM in the text) and a mid-latitude non-axisymmetric positive anomaly (the oval shape, referred to as NAM); (b) The density structure of the inner core at equilibrium (dark grey; equatorial band = AIC; mid-latitude = NAIC), reflecting that of the mantle; (c) The density structure of an axially rotated inner core; (d) The gravitational force on the mid-latitude density of the inner core from the mantle equatorial band results in a torque Γ_1; (e) The gravitational force on the equatorial density of the inner core from the mid-latitude mantle density results in a torque Γ_2; (f) The torques viewed in the equatorial plane, Γ_1 and Γ_2 are equal and opposite and there is no net torque; (g), (h) and (i) same as (d), (e) and (f) but when the inner core is axially rotated. In this case, the torques Γ_1 and Γ_2 do not cancel, resulting in a net torque Γ.

This torque leads to a polar motion, directed at 90° to the right of the net torque Γ in Fig. 4(i).

The total polar motion in consequence to an axial inner core rotation is then the sum of the direct change in the moment of inertia (Fig. 3) and of the subsequent gravitational torque (Fig. 4). These two effect produce polar motions in opposite directions, though they do not cancel one another exactly. Our calculations in the sections that follow indicate that the polar motion from the volume torque exceeds that from the moment of inertia change.

We note that the mechanisms described above rests on the misalignment between the inner core's density structure and the gravitational potential imposed by the mantle. Thus, polar motion occurs only provided the timescale of the axial rotation of the inner core is shorter than its viscous relaxation timescale. Otherwise, the density structure of the inner core would readjust to preserve the hydrostatic equilibrium, yielding no misalignment and no torque.

We have good reasons to believe that decade timescale polar motion based on this mechanism may occur in the Earth. Decadal fluid motions in the core are dominated by azimuthal flows. Torsional oscillations, which are azimuthal oscillations of rigid co-axial cylindrical surfaces, are predicted by theory (Taylor 1963; Braginsky 1970) and observations suggest their presence in the core (Jault *et al.* 1988; Jackson *et al.* 1993; Zatman & Bloxham 1997). Because of the strong radial magnetic field at the ICB, torsional oscillations are expected to entrain the inner core in their motion as a result of electromagnetic tractions (Gubbins 1981). The decadal torsional oscillations are then highly effective at generating oscillations in axial rotation of the inner core, and thus leading to polar motion at a typical timescale of decades.

3.3 Gravitational torque from non-axisymmetric density

The longitudinal direction and amplitude of the equatorial torque pictured in Fig. 4 depends on the details of the mantle density structure and on the amplitude and phase of the axial angular displacement of the inner core. In this section, we present a quantitative description of the torque in terms of these quantities.

The gravitational torque on the inner core is defined by

$$\mathbf{\Gamma}_g = -\int_V \mathbf{r} \times \rho_s \boldsymbol{\nabla}\Phi \, \mathrm{d}V, \tag{5}$$

where the volume V is taken oven the inner core, ρ_s is the inner core density and Φ is the gravitational potential. At hydrostatic equilibrium, contours of ρ_s and Φ coincide and there is no torque. An axial rotation of the inner core induces the longitudinal misalignment between ρ_s and Φ that results in a non-zero $\mathbf{\Gamma}_g$. When the inner core is axially rotated, an additional surface torque occurs as a result of the misalignment of the ICB with surfaces of constant hydrostatic fluid pressure p_s at the bottom of the fluid core,

$$\mathbf{\Gamma}_p = -\int_S p_s \mathbf{r} \times \mathbf{dS}, \tag{6}$$

where the surface S is defined by the ICB. The latter is related to the gravitational force through the hydrostatic balance in the fluid core, $\nabla p_s = -\rho_f' \nabla\Phi$, where ρ_f' is the density of the fluid core at the ICB. The total pressure field includes a dynamic part, however this part is much smaller than the hydrostatic part and we neglect it here. Using Gauss' theorem, the surface integral can be converted into a volume integral, and the total torque on the inner core can be written more simply as

$$\mathbf{\Gamma}_V = -\int_V \mathbf{r} \times (\rho_s - \rho_f')\boldsymbol{\nabla}\Phi \, \mathrm{d}V. \tag{7}$$

Thus, only the part of the inner core density structure in excess of that from a body of similar shape but of constant density ρ_f' is involved in the torque. Although it also includes the effects of fluid pressure on the surface of the inner core, we refer to $\mathbf{\Gamma}_V$ as the gravitational volume torque to simplify the discussion. We note that the surface torque component of (7) should not be confused with the surface torque arising from tractions induced by non-hydrostatic fluid motions.

The amplitude of the torque is a function of the density structure and gravitational potential, and both vary with radius. A detailed derivation of the torque is presented in Appendix A, where we show that it can be written as

$$\tilde{\Gamma}_V = i \sum_{l=1}^{\infty} \sum_{m=0}^{l-1} c_{lm}^{+} I_l^m \xi_l^{m+1*} \left[e^{-im\bar{\phi}} - e^{i(m+1)\bar{\phi}} \right], \tag{8}$$

where we have used

$$\tilde{\Gamma}_V = (\Gamma_V)_1 + i(\Gamma_V)_2 \tag{9}$$

and where the directions 1 and 2 refer to the two equatorial directions of the mantle reference frame. In (8), $\bar{\phi}$ is the longitudinal angle of axial inner core rotation and

$$c_{lm}^{+} = \sqrt{(l-m)(l+m+1)}. \tag{10}$$

The constant ξ_l^{m+1*}, where * indicates complex conjugate, represents the amplitude of the gravitational potential due to density heterogeneities outside the inner core. It is defined as

$$\xi_l^m = -\frac{4\pi G}{2l+1}\left[\overline{\rho\varepsilon}_l^m + \frac{\rho_f' \varepsilon_l^m(a_s)}{a_s^{l-2}}\right], \tag{11}$$

in which G is the gravitational constant, a_s is the mean radius at the ICB, and where

$$\overline{\rho\varepsilon}_l^m = \int_{a_s}^{a_e} \rho_o(a') \frac{\partial}{\partial a'}\left[\frac{\varepsilon_l^m(a')}{a'^{l-2}}\right] \mathrm{d}a', \tag{12}$$

with a_e being the mean radius of the Earth. It is important to stress, as the above expression makes clear, that the gravitational torque is between the inner core and both the fluid core and the mantle, not only the latter; the hydrostatic density adjustment of the fluid core to the mantle mass anomalies participates in the gravitational potential felt by the inner core. The constant I_l^m contains the density structure of the inner core. More precisely, it represents the radially integrated contribution to the torque from the interaction between this density and the gravitational potential from the rest of the Earth,

$$I_l^m = \int_0^{a_s} \rho_o(a') \frac{\partial}{\partial a'}\left[a'^{l+3}\varepsilon_l^m(a')\right] \mathrm{d}a' - \rho_f' a_s^{l+3} \varepsilon_l^m(a_s). \tag{13}$$

In (11), (12) and (13), the coefficients ε_l^m represent the aspherical density structure as defined in (4), except for the case $l = 2$, $m = 0$, where ε_l^m must be replaced by $\epsilon + \varepsilon_2^0$.

The final form of the torque in (8) is consistent with our expectation that there must be an axial misalignment between the inner core and the mantle (i.e. $\bar{\phi} \neq 0$), otherwise the gravitational torque on the inner core vanishes. The only contribution to the torque are from the interaction of the density and gravitational potential of the same harmonic degree, but of order separated by one unit. For example, Y_2^0 with Y_2^1, Y_2^1 with Y_2^2, Y_3^0 with Y_3^1, etc. In the illustrations of Fig. 4, the interaction pictured is clearly that between Y_2^0 with Y_2^1. Thus, even if the mid-latitude mass anomaly in Fig. 4 had been drawn much smaller to represent a more localized heterogeneity, it is nevertheless only the Y_2^1 component of its spherical harmonic expansion that participates in the torque.

The interaction Y_2^0–Y_2^1 also represents the most important part of the torque. This is because the elliptical component dominates the non-spherical density structure. In (8), the term associated with $l = 2$, $m = 0$ is the largest of the summation, and the torque can be approximated as

$$\tilde{\Gamma}_V \simeq i\sqrt{6} I_2^0 \xi_2^{1*}\left(1 - e^{i\bar{\phi}}\right). \tag{14}$$

In this simplified version of the torque, I_2^0 is directly related to the dynamical ellipticity of the inner core,

$$I_2^0 = \int_0^{a_s} \rho_o(a') \frac{\partial}{\partial a'}\left[a'^5 \epsilon(a')\right] \mathrm{d}a' - \rho_f' a_s^5 \epsilon(a_s), \tag{15}$$

$$= -\sqrt{\frac{5}{4\pi}}\left[(C_s - A_s) - (C_s' - A_s')\right], \tag{16}$$

where we have neglected ε_2^0 (assumed $< \epsilon$), and where C_s and A_s are, respectively, the axial and equatorial moments of inertia of the inner core, and C_s' and A_s' the moments of inertia of a body of inner core shape but with a constant density ρ_f'.

3.4 Angular momentum dynamics

The polar motion produced in response to an axial rotation of a non-axisymmetric inner core is governed by the internal angular momentum dynamics between the mantle, fluid core and inner core. The change in the moment of inertia and the subsequent equatorial torque $\tilde{\Gamma}_V$ lead to a misalignment between the geometrical axes of each region and the rotation vector. Once this is the case, additional internal torques are triggered which further alter the angular momentum balance. The misalignment of the elliptical density structure of the inner core with that of the mantle and fluid core results in a gravitational torque that resists further tilting of the inner core. A tilted inner core is also subject to a fluid pressure torque because its elliptical surface is no longer aligned with a surface of constant centrifugal potential. In addition, changes in the rotation vector within each region lead to changes in the centrifugal potential, leading to elastic deformations. These deformations alter the moment of inertia and lead to further changes in the angular momentum balance.

To calculate the evolution of the polar motion resulting from the inner core axial rotation, one must take these internal couplings and elastic deformations into account. Models for these have been developed in the context of the study of Earth's forced nutations, the response of the Earth to the external gravitational torques exerted by the Moon, the Sun and other planets (Sasao *et al.* 1980; Wahr 1981; Mathews *et al.* 1991a; Dehant *et al.* 1993). We calculate the response of the Earth to torques applied on the inner core by adapting the model developed by Mathews *et al.* (1991a) for our present purpose, as was done in Dumberry & Bloxham (2002). For the slow timescales of interest in our study ($\mathrm{d}/\mathrm{d}t \ll \Omega_o$), we show in Appendix C how the evolution of the polar motion due to torques on the inner core can be approximated by a coupled ODE system,

$$\frac{\mathrm{d}}{\mathrm{d}t}\tilde{m} = a_{11}\tilde{m} + a_{12}\tilde{n}_s - \frac{\tilde{\Gamma}_V}{A_m \Omega_o} - \frac{i\Omega_o}{A_m}\tilde{c}_p, \tag{17}$$

$$\frac{\mathrm{d}}{\mathrm{d}t}\tilde{n}_s = a_{21}\tilde{m} + a_{22}\tilde{n}_s - \frac{\tilde{\Gamma}_V + \tilde{\Gamma}_\sigma}{A_s \Omega_o} - \frac{\tilde{\Gamma}_V}{A_m \Omega_o} - \frac{i\Omega_o}{A_m}\tilde{c}_p, , \tag{18}$$

where

$$a_{11} = i\Omega_o\left[\frac{A}{A_m}(e - \kappa) - e_s \alpha_3 \frac{A_s}{A_m}\right], \tag{19}$$

$$a_{12} = i\Omega_o e_s \alpha_3 \alpha_g \frac{A_s}{A_m}, \tag{20}$$

$$a_{21} = i\Omega_o\left[\frac{A}{A_m}(e - \kappa) - e_s \alpha_3\left(1 + \frac{A_s}{A_m}\right)\right], \tag{21}$$

$$a_{22} = i\Omega_o e_s \alpha_3\left(1 + \alpha_g + \alpha_g \frac{A_s}{A_m}\right). \tag{22}$$

In these equations, A is the equatorial moment of inertia of the elliptical Earth, and A_m and A_s are those defined for the mantle and the inner core, e and e_s are the dynamical ellipicities of the whole Earth and the inner core, respectively. The parameters α_3 and α_g are related to the ability of the rest of the Earth to exert a torque on a tilted inner core (see Mathews *et al.* 1991a, for exact definitions) and κ is a compliance factor characterizing elastic deformations that take place under polar motion. The polar motion $\boldsymbol{\omega} = \Omega_o \boldsymbol{m}$ is expressed in the conventional complex notation

$$\tilde{m} = m_1 + i m_2 = (\omega_1 + i\omega_2)/\Omega_o. \tag{23}$$

Similarly,

$$\tilde{n}_s = (n_s)_1 + i(n_s)_2 \tag{24}$$

is the amplitude of the inner core tilt. The volume torque $\tilde{\Gamma}_V$ is that described in (8) and

$$\tilde{\Gamma}_\sigma = (\Gamma_\sigma)_1 + i(\Gamma_\sigma)_2, \tag{25}$$

represents the torque from surface forces applied on the inner core at the ICB. This includes the torque from viscous and electromagnetic tractions. The term that includes $\tilde{c}_p$ in (17) represents the change in the moment of inertia tensor that results directly from the inner core axial rotation. We show in Appendix B how $\tilde{c}_p$ can be expressed as

$$\tilde{c}_p = -\sqrt{\frac{4\pi}{15}}\left(1 - e^{i\tilde{\phi}}\right) I_2^{1*}, \tag{26}$$

with I_2^{1*} being given by its definition in (13).

For $\tilde{\Gamma}_v = \tilde{\Gamma}_\sigma = \tilde{c}_p = 0$, two free modes of precession are found in the system (17–18). One is the familiar Chandler wobble (CW) of an oceanless and elastic Earth, and the second is the inner core wobble (ICW), which is the equivalent of the CW but for the inner core. Their frequencies, expressed in cycles per day, are given by (Mathews *et al.* 1991a,b)

$$\text{CW:} \qquad \sigma_1 \approx \frac{A}{A_m}(e - \kappa), \tag{27}$$

$$\text{ICW:} \qquad \sigma_2 \approx e_s \alpha_3 (1 + \alpha_g). \tag{28}$$

These corresponds to periods of 400 d and 6.6 yr, respectively. These free precessions may participate in the polar motion if they are excited by time-dependent torques on the inner core. For a forcing at decade timescale, resonant excitation of the ICW may increase the amplitude of polar motion (Dumberry & Bloxham 2002).

We allow viscoelastic inner core deformations in our formulation by including a linear decay term to eq. (18),

$$\frac{\mathrm{d}}{\mathrm{d}t}\tilde{n}_s = a_{21}\tilde{m} + \left(a_{22} - \frac{1}{\tau}\right)\tilde{n}_s - \frac{\tilde{\Gamma}_V + \tilde{\Gamma}_\sigma}{A_s \Omega_\mathrm{o}} - \frac{\tilde{\Gamma}_V}{A_m \Omega_\mathrm{o}} - \frac{i\Omega_\mathrm{o}}{A_m}\tilde{c}_p. \tag{29}$$

The constant τ represents the characteristic timescale of viscous deformation, and encompasses the effects of a uniform bulk-viscosity of the inner core on the evolution of the tilt of its figure axis. This is obviously an oversimplification of the anelastic deformations taking place within the inner core. However, our intention is simply to include an approximation of their influence on the resulting polar motion. In any case, it is difficult to justify a more complex prescription because the viscosity of the inner core is poorly known. One could also include anelastic deformations in the mantle in a similar way by including a linear decay term to eq. (17), though here we restrict our investigation to a perfectly elastic mantle.

We note that eqs (17)–(29) include elastic deformations caused by the polar motion (through the parameter κ) but not those caused by the internal density change from the axial rotation and tilt of the inner core. These are considered in a separate study (Dumberry 2007b). Their effect is significant, increasing the change in the moment of inertia for a given axial rotation or tilt by a factor close to 2. We have neglected these elastic deformations in the present study to simplify the discussion and to focus on the polar motion produced by the rigid part of the inner core axial and equatorial rotations.

3.5 Static angular momentum balance

In Dumberry & Bloxham (2002), the static equilibrium angular momentum balance between the mantle, fluid core and inner core was investigated for the case of an applied torque on the inner core due to surface tractions ($\tilde{\Gamma}_\sigma$). Here, we look at the equilibrium balance that arises through a change in the moment of inertia via the term $\tilde{c}_p$ and when the applied torque is solely from gravitational volume forces ($\tilde{\Gamma}_V$).

Let us first investigate the static equilibrium established once an axial rotation of the inner core has taken place. We solve (17) and (29) for a fixed value of $\tilde{c}_p$, and for $\tilde{\Gamma}_V = \tilde{\Gamma}_\sigma = 0$ and $d/dt = 0$ (which also eliminates free precessions). In the absence of viscoelastic deformations ($\tau \to \infty$), we obtain the following relationship between $\tilde{m}$ and $\tilde{n}_s$ by eliminating $\tilde{c}_p$ from the system,

$$\tilde{n}_s = \frac{1}{1 + \alpha_g}\tilde{m}. \tag{30}$$

The coefficient $\alpha_g = 2.175$ represents the effect of gravitational coupling on the equatorial bulge of the inner core by the rest of the Earth. The above equilibrium indicates that under a polar motion $\tilde{m}$ caused by a change in the moment of inertia, were it not for the presence of α_g the geometric axis of the inner core would follow the direction of the global rotation vector. If this was not the the case, there would be an unbalanced centrifugal torque from the fluid pressure at the ICB. The gravitational torque on the inner core through α_g resists a perfect alignment of its geometric figure with the rotation vector, and the misalignment is that for which the gravitational and centrifugal torques are in balance.

The static equilibrium produced by a steady volume torque is found by solving (17) and (29) for a fixed value of $\tilde{\Gamma}_V$, $\tilde{\Gamma}_\sigma = \tilde{c}_p = 0$ and $d/dt = 0$. Again in the absence of viscoelastic deformations ($\tau \to \infty$), this equilibrium implies

$$\tilde{n}_s = \frac{A(e - \kappa)}{A_s \alpha_3 e_s}\tilde{m}. \tag{31}$$

This is the angular momentum balance between the polar offset and the tilted inner core pictured in Fig. 2(b). It implies an inner core tilt of $\sim 0.15^\circ$ to produce a polar motion of 25 mas (or a tilt of $\sim 0.06^\circ$ for a polar motion of 10 mas). Perhaps surprisingly, the equilibrium balance achieved through $\tilde{\Gamma}_V$ is fundamentally different from that achieved through $\tilde{\Gamma}_\sigma$ [see eq. 17 and fig. 2(c) of Dumberry & Bloxham (2002)]. This difference arises as a consequence of the role of the fluid core in the generation of the torque. For a surface torque produced by non-hydrostatic fluid motions, an equal and opposite torque must be applied at the base of the fluid core. The angular momentum of the fluid core must change in response to this torque. In the case of the gravitational volume torque $\tilde{\Gamma}_V$ described in this paper, no equal and opposite volume torque is exerted on the fluid core and the latter plays a passive role in the equatorial angular momentum balance. The reason for this is because over timescales of decades, it is reasonable to assume that deformations in the fluid core are hydrostatic. The inner core tilt leads to a deflection of the equipotential contours in the fluid core, but this is accompanied by a coincident deflection of the density contours. Hydrostatic deformations in the fluid core thus prevent the establishment of a volume torque acting on it. This is explained in further detail in Appendix C.

The balance in eq. (31) was used by Greiner-Mai & Barthelmes (2001) to recover the inner core tilt from the Markowitz wobble. However, one has to be careful as this balance does not include the influence of free precessions. The ICW may indeed play a role in the balance between the inner core tilt and polar motion. In addition, eq. (31) does not include the effects of possible anelastic deformations within the inner core. If we include our prescription of viscoelastic deformations in the above analysis, the static balance

becomes

$$\tilde{n}_s = \frac{A(e-\kappa)}{A_s\left(\alpha_3 e_s + \frac{i}{\Omega_o \tau}\right)}\tilde{m}. \tag{32}$$

For short viscous relaxation timescale τ, the inner core tilt and the polar motion are no longer in the same longitudinal plane: the polar motion is rotated anticlockwise with respect to the direction of the inner core tilt. Physically, this is because the readjustment of the inner core shape towards that of the mantle is equivalent to a rotation. In terms of the balance pictured in Fig. 2(b), this rotation is in the direction out of the page, contributing to an angular momentum perturbation perpendicular to that from the tilt of the inner core. To balance the change in angular momentum from these two effects, the displacement of the rotation vector with respect to the geometric figure of the mantle and fluid core must then comprise a component in the direction into the page, implying that $\tilde{m}$ is rotated anticlockwise with respect to $\tilde{n}_s$.

When the volume torque arises as a result of an axial rotation of the inner core, the effect of both $\tilde{c}_p$ and $\tilde{\Gamma}_V$ occur simultaneously. Each depend on the amplitude of the axial rotation, and as we will see below, they lead to comparable, though not equal, changes in polar motion. The static angular momentum balance between $\tilde{n}_s$ and $\tilde{m}$ is closely approximated by

$$\tilde{n}_s = \frac{A(e-\kappa)}{A_s e_s \alpha_3}\,\gamma\,\tilde{m}. \tag{33}$$

where

$$\gamma = \left\{1 + \frac{i}{e_s \alpha_3 \Omega_o \tau} - \frac{\beta_2}{\beta_1}\left[(1+\alpha_g) + \frac{i}{e_s \alpha_3 \Omega_o \tau}\right]\right\}^{-1}, \tag{34}$$

and

$$\beta_1 = \sqrt{6} I_2^0, \quad \beta_2 = \sqrt{\frac{4\pi}{15}}\Omega_o^2 F_2, \tag{35}$$

and the coefficient F_2 relates I_2^m to ξ_2^m through $I_2^m = F_2\,\xi_2^m$ (see eq. A32). In the absence of viscous relaxation, the expression for γ can be written more simply as

$$\gamma = \left[1 - \frac{\beta_2}{\beta_1}(1+\alpha_g)\right]^{-1}. \tag{36}$$

If $\beta_2 = 0$, which amounts to neglecting the polar motion that arises through $\tilde{c}_p$, one retrieves the balance between $\tilde{m}$ and $\tilde{n}_s$ in (31) when $\tilde{\Gamma}_V$ acts alone. The term $\beta_2(1+\alpha_g)/\beta_1$ in the expression for γ thus represents the ratio of the polar motion due to $\tilde{c}_p$ over that due to $\tilde{\Gamma}_V$. The combination $\beta_2(1+\alpha_g)/\beta_1 \approx 0.711$, indicating that the total polar motion from $\tilde{\Gamma}_V$ is larger than that due to $\tilde{c}_p$, though since they have opposite effects on the polar motion, the effect of $\tilde{c}_p$ reduces the polar motion from $\tilde{\Gamma}_V$ by more than 70 per cent.

While $\tilde{c}_p$ and $\tilde{\Gamma}_V$ have comparable effects on $\tilde{m}$, their respective influence on $\tilde{n}_s$ are very different. The change in moment of inertia through $\tilde{c}_p$ imparts a tilt of the inner core of the same order as the polar motion (from the balance 30), but the volume torque on the inner core generates a tilt which is approximately four orders of magnitude larger than the polar motion (from the balance 31). The resulting inner core tilt is thus almost entirely a consequence of the volume torque, with the effect of $\tilde{c}_p$ contributing only to a small and negligible correction. However, since the polar motion is reduced significantly when both $\tilde{c}_p$ and $\tilde{\Gamma}_V$ are considered, the static angular momentum balance in (33) with γ approximately equal to 3.46 (for $\tau \to \infty$) reflects a smaller polar motion for the same inner core tilt compared to the case when $\tilde{\Gamma}_V$ is considered alone.

4 SIMPLE PREDICTIONS OF POLAR MOTION

Predictions of the polar motion generated by a time-dependent axial inner core rotation are obtained by numerically integrating the coupled eqs (17)–(29) with $\tilde{\Gamma}_V$ given by (14), $\tilde{c}_p$ given by (26) and $\tilde{\Gamma}_\sigma = 0$. The numerical values of all the parameters that enter these equations are taken as those presented in Table 1 of Mathews *et al.* (1991b) for model PREM. Solutions depend on the knowledge of I_2^0 and ξ_2^1, as well as the time-dependent axial angular misalignment $\bar{\phi}(t)$. The parameter I_2^0 is a function of the radial variations in density and ellipticity. Assuming an hydrostatic Earth, these two quantities are related by Clairaut's differential equation (e.g. Jeffreys 1970). I_2^0 can then be obtained from a given model of radial density variations. With PREM (Dziewonski & Anderson 1981), we obtain $I_2^0 = -4.80 \times 10^{30}$ kg m^2. The parameter F_2, which relates I_2^1 to ξ_2^1 through the relation $I_2^m = F_2\,\xi_2^m$ (see eq. A32), is also dependent on the choice of the Earth model. Using PREM, $F_2 = -5.41 \times 10^{38}$ kg m^2 s^2.

The convenience of expressing I_2^{1*} as $F_2 \xi_2^{1*}$ is that now both $\tilde{c}_p$ and $\tilde{\Gamma}_V$ depend on the parameter ξ_2^{1*}. The latter may be obtained from a 3-D model of density in the mantle. We consider two different density models. Model 1 is that of Ishii & Tromp (2001), determined from the splitting functions of free oscillations of the Earth and also constrained by free-air gravity anomalies. This model also includes topography at the CMB, the 660-discontinuity and the surface, which result in surface mass densities and additional contributions to ξ_2^1. Model 2 is that of Simmons *et al.* (2007), a model obtained from simultaneous inversion of seismic data and geodynamic constraints including free-air gravity, internal dynamic topography, tectonic plate divergence and flow-induced excess ellipticity of the CMB (Simmons *et al.* 2006), and that also includes the chemical contribution to the density field. In Table 1, we present the value of ξ_2^1 that we have calculated for each model. We also give the value of $\tilde{\Gamma}_V$ calculated from (14) and the value of $i\Omega_o^2 \tilde{c}_p$ calculated from (26), both based on $\bar{\phi} = 4^\circ$. The amplitude of ξ_2^1 (and, consequently, that of $\tilde{c}_p$ and $\tilde{\Gamma}_V$) in Model 1 is more than 60 times larger than that of Model 2, and they have very different phases. This illustrates how it may difficult to obtain a very reliable estimate of ξ_2^1 from the present-day density models, and consequently, a reliable prediction of the polar motion produced by the combination of $\tilde{c}_p$ and $\tilde{\Gamma}_V$.

Perhaps an even more difficult task is to retrieve the time-dependent axial angular misalignments $\bar{\phi}$ that have taken place in the last century. One possible method involves using the secular variation of the Earth's magnetic field from which one can obtain time-dependent horizontal flows at the surface of the core (e.g. Bloxham & Jackson 1991). If one assumes that the part of the time-dependent azimuthal flow which is axisymmetric represent

Table 1. Parameter values from mantle density models.

Parameter	Model 1	Model 2
$\overline{\rho\varepsilon}_2^1$	$(-3.46 - i\,0.76)$	$(-3.87 - i\,4.05) \times 10^{-2}$
$\rho_f'\,\varepsilon_2^1$	$(-4.88 - i1.07)$	$(-5.45 - i5.70) \times 10^{-2}$
ξ_2^1	$(1.40 + i0.31) \times 10^{-9}$	$(1.56 + i1.63) \times 10^{-11}$
$\tilde{\Gamma}_V$	$(-1.12 + i0.29) \times 10^{21}$	$(-1.21 + i1.36) \times 10^{19}$
$i\Omega_o^2 \tilde{c}_p$	$(2.53 - i0.65) \times 10^{20}$	$(2.75 - i3.09) \times 10^{18}$

Values of $\overline{\rho\varepsilon}_2^1$ and $\rho_f'\,\varepsilon_2^1$ are in units of kg m^{-3}, values of ξ_2^1 are in units of s^{-2}, and values of $\tilde{\Gamma}_V$ and $i\Omega_o^2\,\tilde{c}_p$ are in units of N m. The amplitude of $\tilde{\Gamma}_V$ and $i\Omega_o^2\,\tilde{c}_p$ are calculated from (14) and (26), respectively, and with $\bar{\phi} = 4^\circ$. Models 1 and 2 correspond, respectively, to the mantle density models of Ishii & Tromp (2001) and Simmons *et al.* (2007).

torsional oscillations, this component of the flow extends rigidly inside the core. By making the further assumption that the inner core is axially entrained by torsional oscillations by virtue of a strong electromagnetic coupling, the history of the axial angular displacement of the inner core can then be retrieved from the core surface flows inside the tangent cylinder (e.g Zatman 2003). However, core flows in this region are not well resolved because this is a small surface area of the CMB (about 6.3 per cent). In addition, there may be important temporal variations in the strength of thermal winds inside the tangent cylinder, even at decade timescales, in which case the assumption of purely rigid flows is invalid.

Instead of computing a highly uncertain time-history of $\bar{\phi}$, we consider simple scenarios of axial inner core rotation to illustrate the type of polar motion that may result from it. We consider first a simplified case where no viscoelastic deformations take place ($\tau \to \infty$), and for which a static equilibrium is maintained ($\mathrm{d}/\mathrm{d}t = 0$). We assume that the axial angular displacement of the inner core is periodic with amplitude $\bar{\phi}_\mathrm{o}$, and given by

$$\bar{\phi}(t) = \bar{\phi}_\mathrm{o} \sin(\omega t). \tag{37}$$

In this case, one can relate the polar motion directly to $\bar{\phi}(t)$ by eliminating $\tilde{n}_s$ from (17) to (29) and using (14) and (26). By using the further simplification $e_s\, \alpha_3\, A_s \ll A\,(e-\kappa)\,(1+\alpha_g)$, we obtain

$$\tilde{m} = \frac{\xi_2^{1*}\left[1 - e^{i\bar{\phi}(t)}\right]}{A\Omega_\mathrm{o}^2(e-\kappa)} \left[\frac{\beta_1}{(1+\alpha_g)} - \beta_2\right], \tag{38}$$

where we have used (35). The first and second β terms inside the parenthesis represent the respective contribution of $\tilde{\Gamma}_V$ and $\tilde{c}_p$ to the polar motion.

In Fig. 5(a), we show the polar motion predicted from (38) for a full period of oscillation, $\bar{\phi}_\mathrm{o} = 4^\circ$ and ξ_2^1 from Model 1. The oscillating polar motion follows a trajectory which is a portion of a circular motion, with a distance of arc determined by the amplitude $\bar{\phi}_\mathrm{o}$. For $\bar{\phi}_\mathrm{o} = \frac{\pi}{2}$, the motion would have been a semi-circle, but for small $\bar{\phi}_\mathrm{o}$ the small distance of arc appears to be a quasi-linear trajectory aligned along a specific longitudinal plane. The associated inner core tilt is shown in Fig. 6(a), where the relationship between $\tilde{m}$ and $\tilde{n}_s$ is simply that determined by (33). The extrema in both the polar motion and inner core tilt correspond to the extrema in the axial angular displacement of the inner core.

Fig. 5(a) illustrates how small amplitude, long period, axial oscillations lead to a polar motion polarized along a specific longitudinal plane. Moreover, for the density model of Ishii & Tromp (2001) and with an amplitude of axial inner core oscillation of 4°, this mechanism can generate a polar motion with an amplitude similar to that of the Markowitz wobble pictured in Fig. 1(a). To generate the polar motion of 22 mas of Fig. 5(a), the required amplitude of $\tilde{\Gamma}_V$ and $i\Omega_\mathrm{o}^2\,\tilde{c}_p$ are, respectively, $\sim 1.2 \times 10^{21}$ and $\sim 2.6 \times 10^{20}$ N m, and the associated inner core tilt is $\sim 0.5^\circ$.

We now reinstate the time-derivative terms in (17)–(29), which allows forced oscillations at frequency ω, as well as allowing free precessions to be part of the solution. We also reinstate the effects of viscous deformation of the inner core on the resulting polar motion. The latter influences the solution in three different ways. First, for a given amplitude of axial oscillation of the inner core, it reduces the magnitude of the polar motion generated by $\tilde{c}_p$ and $\tilde{\Gamma}_V$. This is because allowing the rotated density structure of the inner core to relax towards the gravitational potential of the mantle reduces the effective axial misalignment between them and hence the amplitude of both $\tilde{c}_p$ and $\tilde{\Gamma}_V$. For an axial oscillation specified by (37), the axial angle of misalignment as a function of time that enters (26) and (14) is determined by

$$\bar{\phi}(t) = \bar{\phi}_\mathrm{o} \sin(\omega t) - \int_0^t \frac{\bar{\phi}(t')}{\tau}\, \mathrm{d}t'. \tag{39}$$

Secondly, after a tilt of the inner core's geometric figure in response to a torque, viscous relaxation allows the density structure of the inner core to deform towards a realignment of its geometric figure with that of the mantle. The third way in which viscous relaxation affects the resulting polar motion is by attenuating the ICW that may get excited by the torque.

Figs 5(b)–(d) show the polar motions obtained by integrating in time eqs (17)–(29) for three different choices of τ: 100 yr; 10 yr; and 1 yr. Figs 6(b)–(d) show the associated inner core tilt. In all cases, $\bar{\phi}_\mathrm{o} = 4^\circ$, the period of oscillations is 60 yr ($\omega = 2\pi/60\ \mathrm{yr}^{-1}$), ξ_2^1 is from Model 1, and we show the solution for three full periods (180 yr) starting from an initial condition of $\tilde{m} = \tilde{n_s} = 0$. In each of these cases, the resulting polar motion and inner core tilt history is a combination of a forced oscillation from the imposed torque and a free oscillation, the ICW. We note that the CW is also excited due to our choice of initial conditions, but we have removed it from Figs 5(b) to (d) to focus on the longer timescale polar motion. Because we have selected the forcing frequency ω to be different from the frequency of the ICW, no resonance occurs and the ICW does not enhance the amplitude of the forced solution. For all three choices of τ, the ICW is decaying from an initial amplitude set by our choice of initial conditions. For $\tau = 100$ yr (Figs 5b and 6b), the ICW persists for the whole integration time, whereas for $\tau = 10$ yr (Figs 5c and 6c) and $\tau = 1$ yr (Figs 5d and 6d) the ICW is rapidly damped and not re-excited.

The forced polar motion from the imposed inner core oscillation is elliptical and retrograde. The precise ratio of the semi-major and semi-minor axes of the ellipse is a function of the choices of ω and τ. For $\tau = 100$ yr, the polar motion is closer to being circular, though the limit of a highly elliptical shape with the polarisation of Fig. 5(a) can be retrieved by selecting a longer period of oscillation for $\bar{\phi}$. The trajectory of the forced inner core tilt is prograde. As expected, the viscosity of the inner core affects the amplitude of the forced polar motion. For $\tau = 100$ and 10 yr, we retrieve a polar motion of approximately 20 mas, a similar amplitude to the perfectly rigid inner core case of Fig. 5(a). For $\tau = 1$ yr the amplitude is reduced by a factor 2. The amplitude of the inner core tilt is similarly affected by τ; it is approximately 0.5° for $\tau = 100$ yr, 0.4° for $\tau = 10$ yr, and 0.03° for $\tau = 1$ yr. When the viscosity is large, the longitudinal alignment between the semi-major axes of the polar motion and the inner core tilt remains the same as for the perfectly rigid case. For a lower viscosity, the longitudinal direction of the polar motion is rotated in an anticlockwise direction with respect to the longitudinal direction of the inner core tilt, for the reasons described in the previous section. When the viscous relaxation timescale is much shorter than the period of oscillation (Figs 5d and 6d), the offset between the two approaches 90°.

The results of Figs 5(b)–(d) show that it is possible to generate a polar motion with similar attributes to that of the Markowitz wobble with a time-dependent axial inner core rotation. The amplitude, ellipticity and orientation of the resulting polar motion depend on the amplitude and frequency of the axial inner core rotation, the density structure of the mantle, and on the viscosity of the inner core. Some combinations of these parameters lead to a polarized polar motion (e.g. Figs 5c–d) and this mechanism can perhaps explain the general orientation of the Markowitz wobble observed prior to 1976. Of course, some tuning of these parameters would be required in order to reproduce the observed signal more closely. On the other hand, at

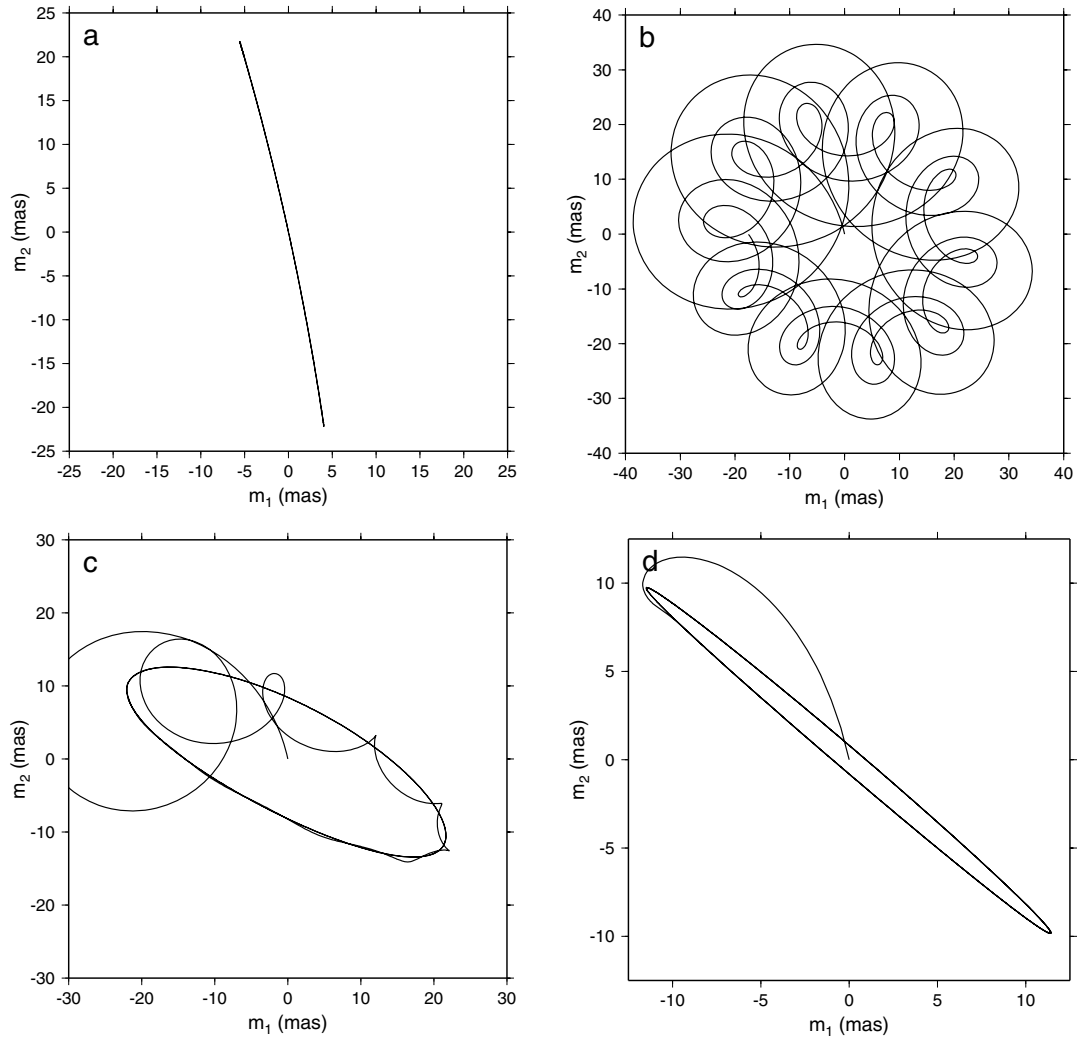

Figure 5. Polar motion resulting from an axially oscillating inner core with a longitudinal amplitude of 4° and a period of 60-yr, and for the mantle density model of Ishii & Tromp (2001). We show the solution for three full periods (180 yr) starting from an initial condition of $\tilde{m} = \tilde{n_s} = 0$. (a) For a rigid inner core and assuming a static equilibrium; (b) For $\tau = 100$ yr; (c) $\tau = 10$ yr and (d) $\tau = 1$ yr.

decadal periods and for a relatively large inner core viscosity, there should be little evidence of polarisation, as exemplified by Fig. 5(b). If the decadal polar motion does not follow a specific polarisation, as the more recent observations suggest, this latter case may provide a more appropriate explanation for the Markowitz wobble.

5 CONSTRAINTS ON THE AMPLITUDE OF THE POLAR MOTION

Using density Model 2 instead of Model 1, solutions that are qualitatively similar to those presented in Figs 5 and 6 are obtained, except that the longitudinal orientation is offset by $\sim 45^\circ$. More importantly though, the predicted amplitude of polar motion and inner core tilt are a factor 60 smaller. Thus, while on the basis of density Model 1 one may conclude that the amplitude of the Markowitz wobble may be explained by the mechanism presented in this study, a very different conclusion is reached with density Model 2. With Model 2, even an amplitude of $\bar{\phi}_o$ as large as 90° would produce a polar motion smaller than the required 10 mas. Moreover, the conclusion that this mechanism may produce a polar motion of 10 mas with Model 1 relies on axial inner core oscillations of at least 2° in amplitude. One may question whether inner core oscillations of such amplitude can actually occur in the Earth's core. To better assess whether this mechanism can explain the Markowitz wobble, it is useful to establish the amplitude of the forced polar motion as a function of the key parameters that directly influences it. Constraints on these parameters can then be used to determine whether a polar motion of 25 mas (or the more modest 10 mas of the past 30 yr) can be realistically produced by an inner core axial rotation.

For the simple prescription of $\phi(t)$ in (39), and when $\bar{\phi}_o \ll 1$, an analytical solution for the forced part of the polar motion can be found and is

$$\tilde{m} = m^{(+)} e^{i\omega t} + m^{(-)} e^{-i\omega t}, \tag{40}$$

where

$$m^{(\pm)} = -\frac{K^{(\pm)}\left[\left(\pm i\omega + \tau^{-1} - i\Omega_o e_s \alpha_3\right)(\beta_1 - \beta_2) + i\Omega_o e_s \alpha_3 \alpha_g \beta_2\right]}{\Omega_o A_m\left[\left(\pm i\omega - a_{11}\right)\left(\pm i\omega + \tau^{-1} - a_{22}\right) - a_{12}a_{21}\right]}, \tag{41}$$

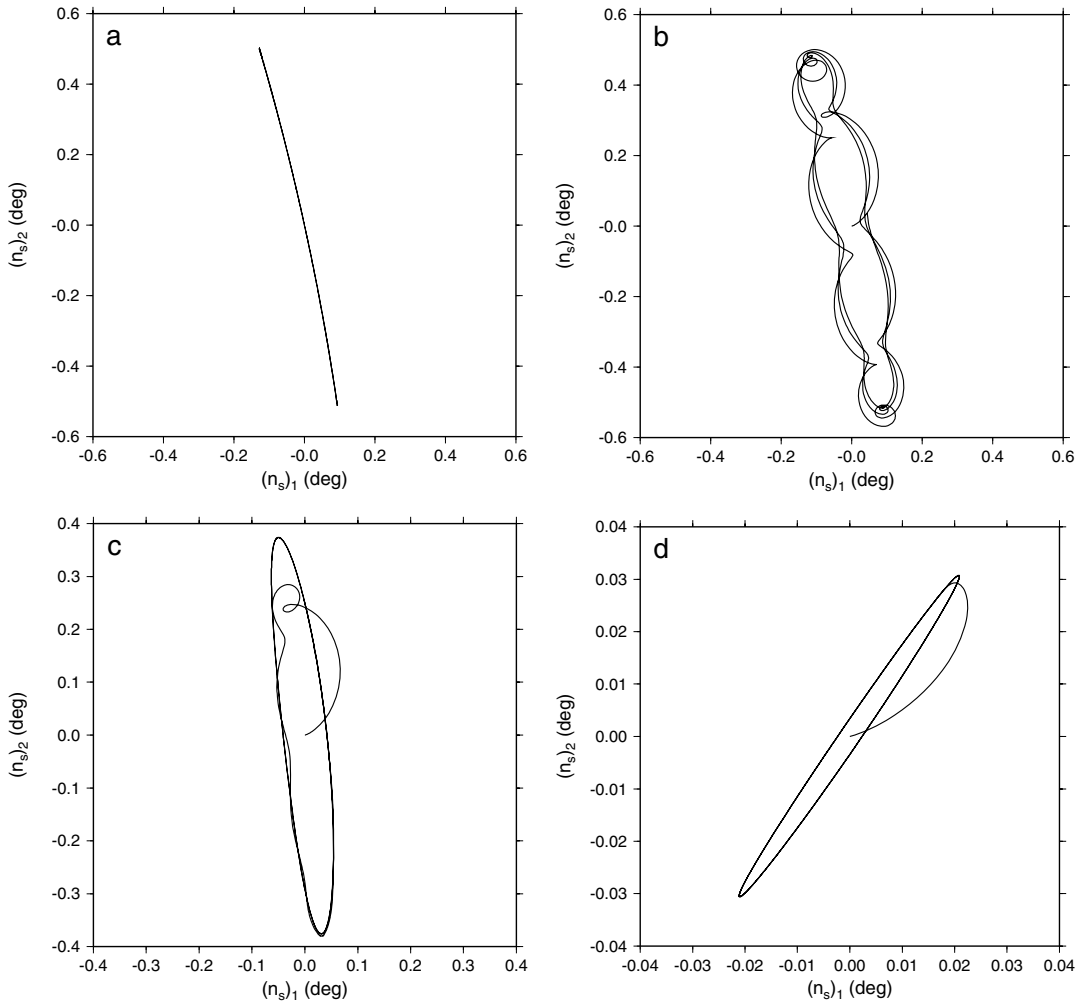

Figure 6. Same as Fig. 5, but showing the inner core tilt. (a) For a rigid inner core and assuming a static equilibrium; (b) For $\tau = 100$ yr; (c) $\tau = 10$ yr and (d) $\tau = 1$ yr.

and the parameter $K^{(\pm)}$ is given by

$$K^{(\pm)} = \frac{\xi_2^{1*}\,\bar{\phi}_o\,\omega}{2\,(\pm i\omega + \tau^{-1})}. \tag{42}$$

In Fig. 7, we show how the amplitude of the forced polar motion varies as a function of τ and the combination $|\xi_2^1|\bar{\phi}_o$. The amplitude is taken as the semi-major axis of the ellipse traced by the polar motion in (40). Once again, we have taken $2\pi/\omega = 60$ yr. The amplitude varies linearly with $|\xi_2^1|$, $\bar{\phi}_o$, and also with τ when $\tau^{-1} \gg \omega$. For $\tau < 1$ yr, the amplitude is well approximated by $6.7 \times 10^3 |\xi_2^1| \bar{\phi}_o \tau$ (in mas). For example, if $\tau = 0.1$ yr (3.16×10^6 s), to achieve an amplitude of 10 mas requires $|\xi_2^1|\bar{\phi}_o \sim 5 \times 10^{-10}$ s^{-2}. For $\tau > 1$ yr, the amplitude of the polar motion remains constant with increasing τ. A lower value $|\xi_2^1|\bar{\phi}_o$ is required in order to produce the same polar motion: to produce an amplitude of $\sim$10 mas, $|\xi_2^1|\bar{\phi}_o$ must be $\sim 5 \times 10^{-11}$ s^{-2}.

Constraints on $|\xi_2^1|$ and $\bar{\phi}_o$ may be obtained from considerations of the axial component of the gravitational torque between the inner core and mantle. As shown in Appendix A, the amplitude of the axial torque on the inner core is determined by the degree 2 density heterogeneity in the mantle,

$$\Gamma_z = -\bar{\Gamma}\,\bar{\phi}(t), \tag{43}$$

where the axial torque coefficient $\bar{\Gamma}$ is given by

$$\bar{\Gamma} = 2|F_2|\left|\xi_2^1\right|^2 + 8|F_2|\left|\xi_2^2\right|^2, \tag{44}$$

where we have used eq. (A40) with $|I_2^m| = |F_2|\,|\xi_2^m|$. A 6-yr oscillation in the LOD has recently been interpreted as the free mode of axial gravitational oscillation between the mantle and the inner core (Mound & Buffett 2003, 2006). If this interpretation is correct, $\bar{\Gamma}$ cannot depart much from 3×10^{20} N m. This constraint implies that, assuming a Y_2^2 component of density equal to zero, the maximum amplitude for $|\xi_2^1|$ is 5.3×10^{-10} s^{-2}. The true maximum value is certain to be smaller than this given that the Y_2^2 component of density, likely of the same order as the Y_2^1 component, contributes four times more to $\bar{\Gamma}$. The amplitude of $|\xi_2^1|$ in Model 2 is smaller than this generous maximum amplitude, however that of Model 1 is a factor $\sqrt{7}$ larger, and violates this constraint.

Using the upper bound of $|\xi_2^1| = 5.3 \times 10^{-10}$ s^{-2}, a polar motion amplitude of 25 mas (10 mas) requires $\bar{\phi}_o \approx 13^\circ (\approx 5^\circ)$. Is this realistic? The axial gravitational torque provides also an upper bound for $\bar{\phi}_o$. An axially oscillating inner core transfers angular momentum to the mantle. This results in axial oscillations of the mantle, though the changes in mantle rotation cannot be larger than the observed changes in LOD. Using a simple model of angular momentum dynamics, Dumberry (2007a) showed that when $\bar{\Gamma} = 3 \times 10^{20}$ N m and $\tau = 5$ yr, the largest rate of rotation of an oscillating inner

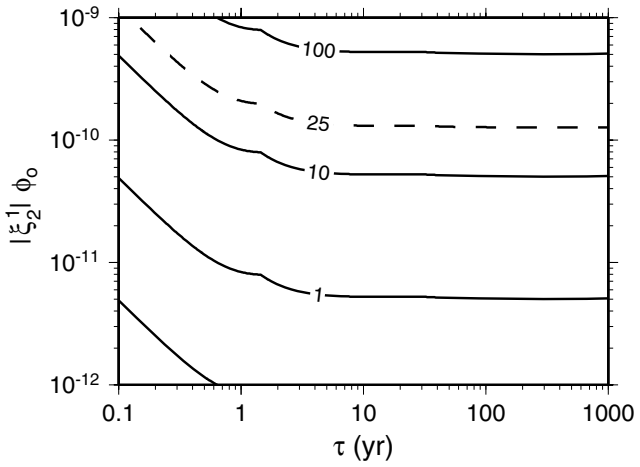

Figure 7. Contours of the amplitude (in mas) of the semi-major axis of the elliptical forced polar molar motion predicted by (40) as a function of the viscous relaxation timescale of the inner core (τ) and the product $|\xi_2^1|\,\bar{\phi}_o$ (in units of s^{-2}). The dashed contour of 25 mas represents the approximate amplitude of the Markowitz wobble observed over the past century.

core at a period of 60 yr is $\Omega_i \sim 0.03^\circ\,\mathrm{yr}^{-1}$. This corresponds to an upper bound in the amplitude of axial angular displacement of $\bar{\phi}_o \sim \Omega_i/\omega \sim 0.3^\circ$. The combination of these upper bounds on $|\xi_2^1|$ and $\bar{\phi}_o$ imply that $|\xi_2^1|\bar{\phi}_o$ cannot be larger than $\sim 3 \times 10^{-12}\ \mathrm{s}^{-2}$. Since the Y_2^2 component of density is likely to explain a large part of $\bar{\Gamma}$, the upper bound is probably closer to $10^{-12}\ \mathrm{s}^{-2}$. Based on Fig. 7, the largest polar motion generated by this mechanism may at most be approximately 0.25 mas (for which the amplitude of the inner core tilt is $\sim 0.005^\circ$). Allowing for elastic deformations associated with the axial rotation and tilt of the inner core density structure would increase the resulting polar motion by a factor close to 2 (Dumberry 2007b), though this remains too small to explain the Markowitz wobble.

If the 6-yr oscillation in LOD is not due to inner core–mantle gravitational coupling, then ξ_2^1 may be as large as its value in Model 1. However, $\bar{\Gamma}$ is proportionally increased, implying that the restriction on $\bar{\phi}_o$ from the observed decadal LOD variation is proportionally decreased; the upper bound on $|\xi_2^1|\bar{\phi}_o$ does not change. Larger values of $\bar{\phi}_o$ are allowed by the decadal LOD variation, but only for a proportional decrease in τ. Since for small τ the amplitude of the polar motion is also proportional to τ, this would not allow larger polar motion to be produced.

Unless the maximum amplitude of inner core oscillation estimated by Dumberry (2007a) is grossly inaccurate, it is difficult to avoid the constraints on ξ_2^1 and $\bar{\phi}_o$ from the axial component of the gravitational torque. In terms of amplitude, the prediction of ξ_2^1 from Model 2 is likely closer to the reality than Model 1. Thus, although the mechanism presented in this study can produce a polar motion that is polarized about a specific longitudinal plane, it is doubtful that its amplitude exceed a fraction of 1 mas. Therefore, it is unlikely that it can explain the Markowitz wobble.

6 CONCLUSION

In this work, we have shown that an axial misalignment between the non-axisymmetric density structures of the mantle and inner core leads to a change in the moment of inertia of the Earth. In addition, this density misalignment results in an equatorial gravitational torque on the inner core, leading to a tilt of its oblate geometric figure and to a further change in the moment of inertia. To conserve angular momentum, an adjustment of the Earth's rotation vector must occur which, in a frame fixed to the mantle, results in a polar motion. The attributes of the polar motion from this mechanism depends on a number of parameters, including the density structure of the mantle (primarily its Y_2^1 density distribution), the rate and angular amplitude of axial inner core rotation, and the bulk viscosity of the inner core.

We have shown that this mechanism can generate a polar motion that tends to be aligned along a preferred longitudinal plane, as is observed for the Markowitz wobble prior to 1976. The plane of polarisation is primarily determined by the Y_2^1 density distribution, though it is also affected by the inner core viscosity. The amplitude of the polar motion generated by this mechanism depends on the amplitude of the Y_2^1 mantle mass anomalies, including topography at density discontinuities, and on the amplitude of the longitudinal misalignment between the density structures of the inner core and mantle. Based on a density model published by Ishii & Tromp (2001), a polar motion of a similar amplitude as that of the observed Markowitz wobble (25 mas) can be achieved with an amplitude of axial inner core oscillation of $\sim 4^\circ$. The smaller amplitude polar motion of 10 mas observed over the last 30 yr requires a smaller amplitude of $\sim 2^\circ$.

However, upper bounds on the amplitude of axial inner core oscillations and on the mantle mass anomalies, both derived from considerations of axial gravitational coupling between the inner core and mantle, suggest that the largest amplitude of polar motion that can be generated by this mechanism is less than 1 mas. This is smaller than the amplitude of the decadal polar motion due to mass redistribution within the atmosphere and ocean, which is of the order of 3 mas (Gross *et al.* 2005). Unless the upper bounds that we have derived are grossly incorrect, it is unlikely that fluctuations in the axial inner core rotation can explain the Markowitz wobble.

It remains possible that the explanation behind the Markowitz wobble involves the inner core, however it must be from a different mechanism than the one presented here. One possibility is that an equatorial torque from electromagnetic surface forces may produce a sufficiently large tilt of the inner core to produce the observed polar motion. Electromagnetic stress at the ICB results predominantly from the shear of the radial magnetic field by horizontal flows. Assuming a purely axisymmetric zonal flow in the core (representing torsional oscillations), a non-rotating inner core and a non-axisymmetric magnetic field at the ICB, Dumberry & Bloxham (2002) concluded that an electromagnetic torque of the correct magnitude (10^{20} N m) is possible. However, strong electromagnetic coupling in the axial direction tend to prevent differential velocity at the ICB: the free modes of torsional oscillations inside the tangent cylinder are restricted to a rigid body rotation and the inner core is axially rotating at the same angular velocity. With little differential rotation at the ICB, the electromagnetic torque from the free modes of torsional oscillations is, therefore, too small, as was shown by Mound (2005).

In order to produce an equatorial electromagnetic torque on the inner core of 10^{20} N m, core flows other than free torsional oscillations must be involved. The torque proposed by Dumberry & Bloxham (2002) may still apply if a different type of zonal flow is also present within the tangent cylinder, for instance a zonal flow with a large differential rotation as a function of cylindrical radius and with significant temporal changes on a decadal timescale. Alternately, changes in the mean meridional flows near the ICB may be important at decade timescales, for instance due to changes in the thermal wind balance. The interaction between this flow and the

magnetic field at the ICB generates an equatorial electromagnetic torque, provided they are not both purely axisymmetric. Finally, it is possible that the torque may not involve a large scale flow, but instead results from the integrated effect of the small-scale interaction between the radial magnetic field and horizontal flows. Despite large spatial cancellations, this torque may be large if convection is vigorous inside the tangent cylinder and changes in local electromagnetic stress occur on a timescale of decades. That any of these mechanism can generate a sufficiently large electromagnetic torque remains speculative, though these ideas are currently being investigated.

ACKNOWLEDGMENTS

I gratefully acknowledge Steve R. Dickman for a thorough review and for pointing out that a polar motion is induced directly by an inner core rotation, an very important point that I had originally overlooked. I also thank Richard S. Gross for sharing his POLE2005 time-series of polar motion. This work was supported by a NERC postdoctoral fellowship of the UK.

REFERENCES

Aurnou, J. & Olson, P., 2000. Control of inner core rotation by electromagnetic, gravitational and mechanical torques, *Phys. Earth planet. Inter.,* **117,** 111–121.

Bloxham, J. & Jackson, A., 1991. Fluid flow near the surface of Earth's outer core, *Rev. Geophys.,* **29,** 97–120.

Braginsky, S.I., 1970. Torsional magnetohydrodynamic vibrations in the Earth's core and variations in day length, *Geomag. Aeron.,* **10,** 1–10.

Buffett, B.A., 1996a. Gravitational oscillations in the length of the day, *Geophys. Res. Lett.,* **23,** 2279–2282.

Buffett, B.A., 1996b. A mechanism for fluctuations in the length of day, *Geophys. Res. Lett.,* **23,** 3803–3806.

Buffett, B.A., 1998. Free oscillations in the length of day: inferences on physical properties near the core–mantle boundary, in *The Core–Mantle Boundary Region*, Vol. 28, pp. 153–165, eds Gurnis, M., Wysession, M.E., Knittle, E. & Buffett, B.A., Geodynamics series, AGU Geophysical Monograph, Washington, DC.

Celaya, M.A., Wahr, J.M. & Bryan, F.O., 1999. Climate-driven polar motion, *J. geophys. Res.,* **104,** 12 813–12 829.

Chao, B.F. & Gross, R.S., 1987. Changes in the earth's rotation and low-degree gravitational field induced by earthquakes, *Geophys. J. R. astr. Soc.,* **91,** 569–596.

Dahlen, F.A. & Tromp, J., 1998. *Theoretical Global Seismology*, Princeton University Press, Princeton, New Jersey.

de Viron, O., Salstein, D., Bizouard, C. & Fernandez, L., 2004. Low-frequency excitation of length of day and polar motion by the atmosphere, *J. geophys. Res.,* **109**(B03408), doi:1029/2003JB002817.

Dehant, V., Hinderer, J., Legros, H. & Lefftz, M., 1993. Analytical approach to the computation of the Earth, the outer core and inner core rotational motions, *Phys. Earth planet. Inter.,* **76,** 259–282.

Dickman, S.R., 1981. Investigation of controversial polar motion features using homogeneous international latitude service data, *J. geophys. Res.,* **86,** 4904–4912.

Dumberry, M., 2007a. Geodynamic constraints on the steady and time-dependent inner core axial rotation, *Geophys. J. Int.,* **170,** 886–895.

Dumberry, M., 2007b. Decadal variations in gravity caused by a tilt of the inner core, *Geophys. J. Int.,* doi:10.1111/j.1365-246X.2007.03624.x.

Dumberry, M. & Bloxham, J., 2002. Inner core tilt and polar motion, *Geophys. J. Int.,* **151,** 377–392.

Dziewonski, A.M. & Anderson, D.L., 1981. Preliminary reference Earth model, *Phys. Earth planet. Inter.,* **25,** 297–356.

Edmonds, A.R., 1960. *Angular Momentum in Quantum Mechanics*, Princeton University Press, New Jersey.

Greff-Lefftz, M. & Legros, H., 1995. Core mantle coupling and polar motion, *Phys. Earth planet. Inter.,* **91,** 273–283.

Greiner-Mai, H. & Barthelmes, F., 2001. Relative wobble of the Earth's inner core derived from polar motion and associated gravity variations, *Geophys. J. Int.,* **144,** 27–36.

Gross, R.S., 2000. Combinations of Earth-orientation measurements: SPACE97, COMB97, and POLE97, *J. Geodesy,* **73,** 627–637.

Gross, R.S. & Vondrák, J., 1999. Astrometric and space-geodetic observations of polar wander, *Geophys. Res. Lett.,* **26,** 2085–2088.

Gross, R.S., Fukumori, I. & Menemenlis, D., 2005. Atmosphere and oceanic excitation of decade-scale Earth orientation variations, *J. geophys. Res.,* **111**((B09405)), doi:10.1029/2004JB003565.

Gubbins, D., 1981. Rotation of the inner core, *J. geophys. Res.,* **86,** 11 695–11 699.

Hide, R., Boggs, D.H., Dickey, J.O., Dong, D., Gross, R.S. & Jackson, A., 1996. Topographic core–mantle coupling and polar motion on decadal time-scales, *Geophys. J. Int.,* **125,** 599–607.

Hulot, G., Le Huy, M. & Le Mouël, J.-L., 1996. Influence of core flows on the decade variations of the polar motion, *Geophys. Atrophys. Fluid Dyn.,* **82,** 35–67.

Ishii, M. & Tromp, J., 2001. Even-degree lateral variations in the Earth's mantle constrained by free oscillations and the free-air gravity anomaly, *Geophys. J. Int.,* **145,** 77–96.

Jackson, A., Bloxham, J. & Gubbins, D., 1993. Time-dependent flow at the core surface and conservation of angular momentum in the coupled core–mantle system, in *Dynamics of the Earth's Deep Interior and Earth Rotation*, Vol. 72, pp. 97–107, eds Le Mouël, J.-L., Smylie, D.E. & Herring, T., AGU Geophysical Monograph, Washington, DC.

Jault, D., Gire, C. & Le Mouël, J.-L., 1988. Westward drift, core motions and exchanges of angular momentum between core and mantle, *Nature,* **333,** 353–356.

Jeffreys, H., 1970. *The Earth*, 5th edn, Cambridge University Press, London, UK.

Lambeck, K., 1980. *The Earth's Variable Rotation: Geophysical Causes and Consequences*, Cambridge University Press, Cambridge.

Markowitz, W., 1960. Latitude and longitude and the secular motion of the pole, in *Methods and Techniques in Geophysics*, pp. 325–361, ed. Runcorn, S.K., Interscience Publishers, London.

Markowitz, W., 1968. Concurrent astronomical observations for studying continental drift, polar motion, and the rotation of the Earth, in *Continental Drift, Secular Motion of the Pole and Rotation of the Earth*, pp. 25–32, eds Markowitz, W. & Guinot, B., Springer-Verlag, Dordrecht.

Mathews, P.M., Buffett, B.A., Herring, T.A. & Shapiro, I.I., 1991a. Forced nutations of the Earth: influence of inner core dynamics. 1. theory, *J. geophys. Res.,* **96,** 8219–8242.

Mathews, P.M., Buffett, B.A., Herring, T.A. & Shapiro, I.I., 1991b. Forced nutations of the Earth: influence of inner core dynamics. 2. numerical results, *J. geophys. Res.,* **96,** 8243–8257.

Mound, J.E., 2005. Electromagnetic torques in the core and resonant excitation of decadal polar motion, *Geophys. J. Int.,* **160,** 721–728.

Mound, J.E. & Buffett, B.A., 2003. Interannual oscillations in the length of day: implications for the structure of mantle and core, *J. geophys. Res.,* **108**(B7), 2334, doi:10.1029/2002JB002054.

Mound, J.E. & Buffett, B.A., 2005. Mechanisms of core–mantle angular momentum exchange and the observed spectral properties of torsional oscillations, *J. geophys. Res.,* **110,** B08103, doi:10.1029/2004JB003555.

Mound, J.E. & Buffett, B.A., 2006. Detection of a gravitational oscillation in length-of-day, *Earth planet. Sci. Lett.,* **243,** 383–389.

Munk, W.H. & MacDonald, G.J.F., 1960. *The Rotation of the Earth*, Cambridge University Press, Cambridge.

Poma, A., Proverbio, E. & Uras, S., 1987. Long term variations in the Earth's motion and crustal movements, *J. Geodyn.,* **8,** 245–261.

Ponte, R.M., Rajamony, J. & Grogory, J.M., 2002. Ocean angular momentum signals in a climate model and implications for Earth rotation, *Clim. Dyn.,* **19,** 181–190.

Sasao, T., Okubo, T. & Saito, M., 1980. A simple theory on the dynamical effects of a stratified fluid core upon nutational motion of the Earth, in *Proceedings of IAU Symposium*, Vol. 78, pp. 165–183, eds Federov, E.P., Smith, M.L. & Bender, P.L., D., Reidel, Hingham, Mass.

Simmons, N.A., Forte, A.M. & Grand, S.P., 2006. Constraining mantle flow with seismic and geodynamic data: a joint approach, *Earth planet. Sci. Lett.,* **246,** 109–124.

Simmons, N.A., Forte, A.M. & Grand, S.P., 2007. Thermochemical structure and dynamics of the African superplume, *Geophys. Res. Lett.,* **34,** L02301, doi:10.1029/2006GL028009.

Stevenson, D.J., 1987. Limits on lateral density and velocity variations in the Earth's core, *Geophys. J. R. astr. Soc.,* **88,** 311–319.

Taylor, J.B., 1963. The magneto-hydrodynamics of a rotating fluid and the Earth's dynamo problem, *Proc. R. Soc. Lond., A,* **274,** 274–283.

Vicente, R.O. & Currie, R.G., 1976. Maximum entropy spectrum of long-period polar motion, *Geophys. J. R. astr. Soc.,* **46,** 67–73.

Vicente, R.O. & Wilson, C.R., 2002. On long-period polar motion, *J. Geodesy,* **76,** 199–208.

Vondrák, J., 1999. Earth rotation parameters 1899.7–1992.0 after reanalysis within the Hipparcos frame, *Surv. Geophys.,* **20,** 169–195.

Wahr, J.M., 1981. The forced nutations of an ellitical, rotating, elastic and oceanless Earth, *Geophys. J. R. astr. Soc.,* **87,** 633–668.

Wilson, C.R. & Vicente, R.O., 1980. An analysis of homogeneous ILS polar motion series, *Geophys. J. R. astr. Soc.,* **62,** 605–616.

Xu, S., Crossley, D. & Szeto, A.M.K., 2000. Variations in length of day and inner core differential rotation from gravitational coupling, *Phys. Earth planet. Inter.,* **117,** 95–110.

Zatman, S., 2003. Decadal oscillations of the Earth's core, angular momentum exchange, and inner core rotation, in *Earth's Core: Dynamics, Structure, Rotation*, Vol. 31, pp. 233–240, eds Dehant, V., Creager, K.C., Karato, S.-I. & Zatman, S., Geodynamics series, AGU Geophysical Monograph.

Zatman, S. & Bloxham, J., 1997. Torsional oscillations and the magnetic field within the Earth's core, *Nature,* **388,** 760–763.

APPENDIX A: DETERMINATION OF THE TORQUE Γ_V

The gravitational torque on the inner core is determined by eq. (7)

$$\mathbf{\Gamma}_V = -\int_V (\rho_s - \rho_f')\,\mathbf{r}\times\boldsymbol{\nabla}\Phi\,\mathrm{d}V. \tag{A1}$$

Since

$$\mathbf{r}\times\boldsymbol{\nabla} = \hat{\mathbf{e}}_r\times\boldsymbol{\nabla}_1 = -\hat{\mathbf{e}}_\theta\frac{1}{\sin\theta}\frac{\partial}{\partial\phi} + \hat{\mathbf{e}}_\phi\frac{\partial}{\partial\theta}, \tag{A2}$$

where $(r,\ \theta,\ \phi)$ are spherical coordinates with unit vectors $(\hat{\mathbf{e}}_r, \hat{\mathbf{e}}_\theta, \hat{\mathbf{e}}_\phi)$, it is clear that only the laterally varying part of the gravitational potential is involved in the torque.

The gravitational potential inside the inner core can be separated into a sum of two parts,

$$\Phi = \Phi^{(\mathrm{MF})} + \Phi^{(\mathrm{SIC})}. \tag{A3}$$

The part $\Phi^{(\mathrm{MF})}$ is that due to density heterogeneities external to the inner core. It includes the gravitational potential due to the mass anomalies in the mantle, and also that from the hydrostatic density adjustment in the fluid that results from the presence of these mass anomalies. Assuming its viscosity to be smaller than that of the mantle, the inner core can be regarded as a fluid, and just as it is the case for the fluid core, its surfaces of constant density also deform to match the imposed external potential. The inner core density perturbation from this effect is responsible for the gravitational potential $\Phi^{(\mathrm{SIC})}$.

The part of the inner core density structure that participates in the torque involves also ρ_f'. It is convenient to introduce $\Phi^{(\mathrm{SIC}')}$, the gravitational potential due to a body of inner core shape and constant density ρ_f'. The total potential inside the inner core (A3) can be written as

$$\Phi = \Phi^{(\mathrm{MF})} + \Phi^{(\mathrm{SIC})} - \Phi^{(\mathrm{SIC}')} + \Phi^{(\mathrm{SIC}')}. \tag{A4}$$

When the inner core is axially rotated, it involves both ρ_s and ρ_f'. The axially rotated density may be written as $(\tilde{\rho}_s - \tilde{\rho}_f')$, and the gravitational potential associated with it is also rotated. The total potential inside the inner core when the latter is axially rotated is

$$\Phi = \Phi^{(\mathrm{MF})} + \Phi^{(\mathrm{SIC}')} + \left[\tilde{\Phi}^{(\mathrm{SIC})} - \tilde{\Phi}^{(\mathrm{SIC}')}\right]. \tag{A5}$$

The rotated part of the potential does not participate in the torque in (A1) since, by definition, it has remained aligned with the rotated density structure. The torque only involves the part of the potential which remains fixed with respect to the mantle,

$$\mathbf{\Gamma} = -\int_V (\tilde{\rho}_s - \tilde{\rho}_f')\mathbf{r}\times\boldsymbol{\nabla}\left[\Phi^{(\mathrm{MF})} + \Phi^{(\mathrm{SIC}')}\right]\mathrm{d}V. \tag{A6}$$

The gravitational potential of a slightly non-spherical body whose surfaces of constant density are defined according to (4) is well known (Jeffreys 1970). At interior points $\mathbf{r} = (r,\theta,\phi)$, it is obtained by adding together the separate contribution due to mass inside and outside of a_r (the mean spherical radius at r),

$$\begin{aligned}\Phi(\mathbf{r}) = &-4\pi G\left[\int_{a_r}^{a}\rho_{\mathrm{o}}(a')a'\mathrm{d}a' + \frac{1}{r}\int_0^{a_r}\rho_{\mathrm{o}}(a')a'^2\mathrm{d}a'\right]\\ &-\sum_{1,m}\frac{4\pi G}{2l+1}\left[\frac{1}{r^{l+1}}\int_0^{a_r}\rho_{\mathrm{o}}(a')\frac{\partial}{\partial a'}a'^{l+3}\varepsilon_l^m(a')\,\mathrm{d}a'\right]Y_l^m\\ &-\sum_{1,m}\frac{4\pi G}{2l+1}\left[r^l\int_{a_r}^{a}\rho_{\mathrm{o}}(a')\frac{\partial}{\partial a'}\frac{\varepsilon_l^m(a')}{a'^{l-2}}\,\mathrm{d}a'\right]Y_l^m,\end{aligned} \tag{A7}$$

where G is the gravitational constant and a is the external radius of the Earth.

From this general representation of the gravitational potential, it is straightforward to calculate $\Phi^{(\mathrm{MF})}$ and $\Phi^{(\mathrm{SIC}')}$ at any point inside the inner core. The first term on the right hand side of (A7) is the spherically symmetric part of the potential. This part does not participate in the torque, so we are not including it. The gravitational potential $\Phi^{(\mathrm{MF})}$ involves only the mass outside of the inner core with radius a_s, so only the last term of (A7) participates. We write it as

$$\Phi^{(\mathrm{MF})}(\mathbf{r}) = -4\pi G\sum_{l,m}\frac{r^l}{2l+1}\overline{\rho\varepsilon}_l^m Y_l^m, \tag{A8}$$

where $\overline{\rho\varepsilon}_l^m$ is a defined as

$$\overline{\rho\varepsilon}_l^m = \int_{a_s}^{a}\rho_{\mathrm{o}}(a')\frac{\partial}{\partial a'}\left[\frac{\varepsilon_l^m(a')}{a'^{l-2}}\right]\mathrm{d}a'. \tag{A9}$$

The part $\Phi^{(\mathrm{SIC}')}$ can be determined in a similar way. Since ρ_f' is a constant, there is no contribution to the non-spherical gravitational potential from the mass inside a_r. The contribution from the mass outside of a_r can be determined by replacing $\rho_{\mathrm{o}}(a')$ with the constant ρ_f' in the last term of (A7), and also replacing the upper limit of integration by a_s. ρ_f' can be taken out of the integral, and $\Phi^{(\mathrm{SIC}')}$ can be written as

$$\Phi^{(\mathrm{SIC}')}(\mathbf{r}) = -4\pi G\sum_{l,m}\frac{r^l}{2l+1}\frac{\rho_f'\varepsilon_l^m(a_s)}{a_s^{l-2}}Y_l^m. \tag{A10}$$

This is equivalent to the gravitational potential due to an infinitesimally small film with surface density $\rho_f'\ a_s\ \varepsilon_l^m(a_s)$.

The gravitational potential involved in the torque can thus be written as

$$\Phi^{(\mathrm{MF})}(\mathbf{r}) + \Phi^{(\mathrm{SIC}')}(\mathbf{r}) = \sum_{l,m} r^l\xi_l^m Y_l^m, \tag{A11}$$

where the constant ξ_l^m is given by

$$\xi_l^m = -\frac{4\pi G}{2l+1}\left[\overline{\rho\epsilon}_l^m + \frac{\rho_f'\varepsilon_l^m(a_s)}{a_s^{l-2}}\right]. \tag{A12}$$

The evaluation of the torque is carried through by inserting (A11) into (A6),

$$\begin{aligned}\mathbf{\Gamma} &= \sum_{l,m}\int_V (\tilde{\rho}_s - \tilde{\rho}'_f)\mathbf{r}\times\boldsymbol{\nabla}(r^l \xi_l^m Y_l^m)\,\mathrm{d}V,\\ &= \sum_{l,m}\int_\Omega \left[\int_0^{a_s}(\tilde{\rho}_s - \tilde{\rho}'_f) r^{2+l}\mathrm{d}r\right]\xi_l^m(\mathbf{r}\times\boldsymbol{\nabla}Y_l^m)\,\mathrm{d}\Omega, \end{aligned} \tag{A13}$$

where Ω is the surface of the unit sphere. The integral over the deformed surfaces r, which are defined according to (4), is evaluated by a change of variable from r to a', with the first order expansion

$$r^{2+l} = a'^{2+l}\left[1 + (2+l)\sum_{l',m'}\varepsilon_{l'}^{m'}(a')\,Y_{l'}^{m'}\right], \tag{A14}$$

and

$$\mathrm{d}r = \frac{\partial r}{\partial a'}\mathrm{d}a' = \mathrm{d}a' + \sum_{l',m'}\left[\varepsilon_{l'}^{m'}(a') + a'\frac{\partial}{\partial a'}\varepsilon_{l'}^{m'}(a')\right]Y_{l'}^{m'}\mathrm{d}a'. \tag{A15}$$

Keeping only the terms that are first order in $\varepsilon_{l'}^{m'}$, the integral over r can be expanded as

$$\begin{aligned}\int_0^{a_s}(\tilde{\rho}_s - \tilde{\rho}'_f)r^{2+l}\mathrm{d}r \;&=\; \int_0^{a_s}(\rho_s(a') - \rho'_f)a'^{2+l}\mathrm{d}a'\\ &+\sum_{l',m'}\left\{\int_0^{a_s}\rho_s(a')\frac{\partial}{\partial a'}\left[a'^{l+3}\tilde{\varepsilon}_{l'}^{m'}(a')\right]\mathrm{d}a'\right\}Y_{l'}^{m'}\\ &-\sum_{l',m'}\rho'_f a_s^{l+3}\tilde{\varepsilon}_{l'}^{m'}(a_s)Y_{l'}^{m'}, \end{aligned} \tag{A16}$$

where the rotation of the density structure is now carried by $\tilde{\varepsilon}_{l'}^{m'}(a')$. In terms of the non-rotated density structure, the later is simply

$$\tilde{\varepsilon}_{l'}^{m'}(a') = \varepsilon_{l'}^{m'}(a')e^{-im'\bar{\phi}}, \tag{A17}$$

where $\bar{\phi}$ is the angle of axial inner core rotation.

The first term on the right hand side of (A16) is spherically symmetric and does not participate in the torque. Using (A16) and (A17) into (A13), the torque on the inner core can be written as

$$\mathbf{\Gamma} = -\sum_{l,m}\sum_{l',m'} I_{ll'}^{m'}\xi_l^m e^{-im'\bar{\phi}}\int_\Omega Y_{l'}^{m'}(\mathbf{r}\times\boldsymbol{\nabla}Y_l^m)\,\mathrm{d}\Omega, \tag{A18}$$

where

$$I_{ll'}^{m'} = \int_0^{a_s}\rho_s(a')\frac{\partial}{\partial a'}\left[a'^{l+3}\varepsilon_{l'}^{m'}(a')\right]\mathrm{d}a' \;-\rho'_f a_s^{l+3}\varepsilon_{l'}^{m'}(a_s). \tag{A19}$$

To evaluate the integral over the unit sphere, we make use of the angular momentum operator (Edmonds 1960; Dahlen & Tromp 1998)

$$\mathbf{L} = -i(\mathbf{r}\times\boldsymbol{\nabla}), \tag{A20}$$

so that

$$\int_\Omega Y_{l'}^{m'}(\mathbf{r}\times\boldsymbol{\nabla}Y_l^m)\,\mathrm{d}\Omega \;= i\int_\Omega Y_{l'}^{m'}(\mathbf{L}Y_l^m)\,\mathrm{d}\Omega. \tag{A21}$$

This is convenient because the torque in the equatorial direction, which is usually written in complex notation as

$$\tilde{\Gamma} = \Gamma_x + i\Gamma_y, \tag{A22}$$

$$= -i\sum_{l,m}\sum_{l',m'} I_{ll'}^{m'}\xi_l^m e^{-im'\bar{\phi}}\int_\Omega Y_{l'}^{m'}(L_+Y_l^m)\,\mathrm{d}\Omega, \tag{A23}$$

involves the well known ascending ladder operator L_+,

$$L_+ = L_x \;+\; iL_y. \tag{A24}$$

This operator transforms Y_l^m into Y_l^{m+1} according to

$$L_+Y_l^m = c_{lm}^+\,Y_l^{m+1}, \tag{A25}$$

where c_{lm}^+ is a constant defined as

$$c_{lm}^+ = \sqrt{(l-m)(l+m+1)}. \tag{A26}$$

The torque can be written in terms of an integral over the unit sphere involving a product of spherical harmonics,

$$\tilde{\Gamma} = -i\sum_{l,m}\sum_{l',m'}(-1)^{m'}c_{lm}^+ I_{ll'}^{m'}\xi_l^m e^{-im'\bar{\phi}}\int_\Omega Y_{l'}^{-m'*}\,Y_l^{m+1}\,\mathrm{d}\Omega, \tag{A27}$$

where we have used

$$Y_l^m = (-1)^m Y_l^{-m*} \tag{A28}$$

and where* denotes complex conjugate. Following the orthogonality rules for spherical harmonics and the normalisation defined in (3), the only non-zero contribution to the torque are those for which $l = l'$ and $m = -m' - 1$. We can then write the torque in terms of a summation over indices l and m only

$$\tilde{\Gamma} = -i\sum_{l=1}^{\infty}\sum_{m=-l}^{l-1}(-1)^m c_{lm}^+ I_l^m \xi_l^{-m-1}e^{-im\bar{\phi}}, \tag{A29}$$

where the coefficients I_l^m correspond to the coefficients $I_{ll'}^m$ with $l = l'$. By using the fact that the coefficients ξ_l^m are those of a purely real function expanded in complex spherical harmonics, and therefore that

$$\xi_l^{-m} = (-1)^m\xi_l^{m*}, \tag{A30}$$

and similarly for the coefficients I_l^m, the summation can be written in terms of positive values of m,

$$\tilde{\Gamma} = i\sum_{l=1}^{\infty}\sum_{m=0}^{l-1}c_{lm}^+\left[I_l^m\xi_l^{m+1*}e^{-im\bar{\phi}} \;-\; I_l^{m+1*}\xi_l^m e^{i(m+1)\bar{\phi}}\right]. \tag{A31}$$

This expression can be further simplified. Assuming that the inner core is in hydrostatic equilibrium prior to its axial rotation, then I_l^m, which determines its density structure, should be proportional to ξ_l^m, which is a measure of the imposed potential from the mass anomalies in the mantle. The relationship between I_l^m and ξ_l^m is a function of the harmonic degree l, and without specifying the exact relationship, we can write

$$I_l^m = \xi_l^m F_l. \tag{A32}$$

Therefore,

$$I_l^{m+1*}\xi_l^m = \left(F_l\xi_l^{m+1*}\right)\left(\frac{I_l^m}{F_l}\right) = I_l^m\xi_l^{m+1*}, \tag{A33}$$

and (A31) can be simplified to

$$\tilde{\Gamma} = i\sum_{l=1}^{\infty}\sum_{m=0}^{l-1}c_{lm}^+ I_l^m\xi_l^{m+1*}\left[e^{-im\bar{\phi}} \;-\; e^{i(m+1)\bar{\phi}}\right]. \tag{A34}$$

Although some of the steps involved in its derivation may not have been very illuminating in terms of physical processes, the final form of the torque in (A34) is quite straightforward. As expected, unless there is an axial misalignment between the inner core and the mantle (i.e. $\bar{\phi} \neq 0$), the gravitational torque on the inner core vanishes. When there is a misalignment, the torque depends on the amplitude

of the gravitational potential from mantle mass (ξ_l^{m+1*}) and the amplitude of the inner core density structure (I_l^m). Perhaps less intuitive is the fact that the only contributions to the torque arise from the interaction of the density and gravitational potential of the same harmonic degree, but separated by one unit in order.

Finally, if one is interested in the axial part of the torque Γ_z, it can be obtained using the above formalism. From (A18), with (A20) but using the axial part of the angular momentum operator,

$$L_z Y_l^m = m Y_l^m, \tag{A35}$$

the axial component of the torque can be written as

$$\Gamma_z = -i \sum_{l,m} \sum_{l',m'} m(-1)^{m'} I_{ll'}^{m'} \xi_l^m e^{-im'\bar{\phi}} \int_\Omega Y_{l'}^{-m'*} Y_l^m \, \mathrm{d}\Omega, \tag{A36}$$

where we have used (A28). The torque is non-zero only for $l = l'$ and $m = -m'$, and thus

$$\Gamma_z = -i \sum_{l,m} m(-1)^m I_l^{-m} \xi_l^m e^{im\bar{\phi}}. \tag{A37}$$

Using (A30), (A33) and expanding the above result in terms of positive values of m, we get

$$\begin{aligned}\Gamma_z &= -i \sum_{l=1}^{\infty} \sum_{m=1}^{l} m I_l^m \xi_l^{m*} (e^{im\bar{\phi}} - e^{-im\bar{\phi}}), \\ &= 2 \sum_{l=1}^{\infty} \sum_{m=1}^{l} m I_l^m \xi_l^{m*} \sin(m\bar{\phi}).\end{aligned} \tag{A38}$$

For small angular displacements of the inner core, $\sin(m\bar{\phi}) \approx m\bar{\phi}$, and the axial component of the torque simplifies to

$$\Gamma_z = 2 \sum_{l=1}^{\infty} \sum_{m=1}^{l} m^2 I_l^m \xi_l^{m*} \bar{\phi}. \tag{A39}$$

Making use of (A33), we can write an equivalent expression,

$$\Gamma_z = -2 \sum_{l=1}^{\infty} \sum_{m=1}^{l} m^2 \left| I_l^m \right| \left| \xi_l^m \right| \bar{\phi}, \tag{A40}$$

where $|\,|$ denotes the amplitude of the complex coefficients.

Expressions for the axial torque on the inner core when the non-axisymmetric mantle density anomaly is dominated by $l = 2$, $m = 2$ have previously been published by Buffett (1996a) and Xu *et al.* (2000). To write our result in a form suitable for a comparison with the results obtained by these authors, we use

$$|I_2^2| = \frac{1}{2} \sqrt{\frac{15}{8\pi}} \left| (B_s - A_s) - (B'_s - A'_s) \right|, \tag{A41}$$

where $B_s - A_s$ is the difference between the equatorial moments of inertia of the inner core, which, for our definition of r in (4), is defined as

$$B_s - A_s = 2 \sqrt{\frac{8\pi}{15}} \int_0^{a_s} \rho_o(a') \frac{\partial}{\partial a'} \left[a'^5 \varepsilon_2^2(a') \right] \mathrm{d}a'. \tag{A42}$$

The term $B'_s - A'_s$ is obtained by replacing $\rho_o(a')$ with the constant ρ'_f and thus represents the difference between the equatorial moments of a body of inner core shape but with constant density ρ'_f. To be compatible with the published result, we must also write ξ_l^m in terms of the equatorial ellipticity ϵ_e,

$$\left| \xi_2^2 \right| = \frac{4\pi G}{5} \frac{1}{2} \sqrt{\frac{8\pi}{15}} \left| \overline{\rho \epsilon_e} + \rho'_f \epsilon_e(a_s) \right|, \tag{A43}$$

with

$$\overline{\rho \epsilon_e} = \int_{a_s}^{a} \rho_o(a') \frac{\partial \epsilon_e(a')}{\partial a'} \mathrm{d}a', \tag{A44}$$

and where ϵ_e is related to ε_2^2 by

$$\varepsilon_2^2 = \frac{1}{2} \sqrt{\frac{8\pi}{15}} \epsilon_e. \tag{A45}$$

Using (A41) and (A43) in (A39), we obtain

$$\Gamma_z = -\frac{8\pi G}{5} |\overline{\rho \epsilon_e} + \rho'_f \epsilon_e(a_s)| \, |(B_s - A_s) - (B'_s - A'_s)| \bar{\phi}. \tag{A46}$$

The above expression is identical to that obtained by Xu *et al.* (2000). It is smaller by a factor 2 from the value found by Buffett (1996a), has had been pointed out by Xu *et al.* (2000).

APPENDIX B: CHANGE IN THE MOMENT OF INERTIA TENSOR FROM AN AXIAL INNER CORE ROTATION

The axial rotation of the non-axisymmetric inner core leads to an internal mass reorganisation and, consequently, to a change in the moment of inertia tensor of the whole Earth. Since angular momentum must be conserved, an adjustment of the rotation vector takes place which, in a frame of reference fixed to the mantle, results in a polar motion. To take this effect into account in our formalism, we need to determine the changes in moment of inertia induced by an axial inner core rotation.

Using the generalized MacCullagh's formula (Chao & Gross 1987), a change in the moment of inertia tensor is related to the change in the gravitational potential of degree 2. For our choice of normalisation, the following relationship holds

$$\tilde{c}_p = \Delta I_{13} + i \Delta I_{23} = -\sqrt{\frac{5}{12\pi}} \frac{a_e^3}{G} \left(\delta \phi_2^1 \right)^*, \tag{B1}$$

where ΔI_{13} and ΔI_{23} are non-diagonal elements of the moment of inertia tensor, and $(\delta \phi_2^1)^*$ is the complex conjugate coefficient of the change in gravitational potential measured at the surface of the Earth. The latter is caused by the axial rotation of the non-axisymmetric inner core with respect to the mantle frame, and following the notation in Appendix A, it is given by

$$\Delta \Phi = \left[\tilde{\Phi}^{(\mathrm{SIC})} - \tilde{\Phi}^{(\mathrm{SIC}')} \right] - \left[\Phi^{(\mathrm{SIC})} - \Phi^{(\mathrm{SIC}')} \right]. \tag{B2}$$

Using (A7) and (A17), we can write the change in spherical harmonic coefficients of degree 2 at the surface as

$$\delta \phi_2^m = -\frac{4\pi G}{5} \frac{(e^{-im\bar{\phi}} - 1)}{a_e^3} \int_0^{a_s} (\rho_s - \rho'_f) \frac{\partial}{\partial a'} a'^5 \varepsilon_l^m(a') \, \mathrm{d}a', \tag{B3}$$

which, using the definition of I_l^m in (13), can be written more concisely as

$$\delta \phi_2^m = -\frac{4\pi G}{5} \frac{(e^{-im\bar{\phi}} - 1)}{a_e^3} I_2^m. \tag{B4}$$

Substituting (B4) in (B1), we arrive at

$$\tilde{c}_p = \sqrt{\frac{4\pi}{15}} (e^{i\bar{\phi}} - 1) I_2^{1*}. \tag{B5}$$

This last expression represents the change in the moment of inertia of the whole Earth in response to an axial rotation of the inner core of amplitude $\bar{\phi}$.

APPENDIX C: INTERNAL ANGULAR MOMENTUM DYNAMICS

The coupled eqs (17)–(18) govern the polar motion and inner core tilt that result from a prescribed torque applied to the inner core.

They are obtained from a model of the internal angular momentum balance developed for the study of the forced nutations. This model is described in details in Mathews *et al.* (1991a). We give here only a brief description of the model and refer the interested reader to the original paper.

The nutation model describes the internal coupling dynamics of an axisymmetric, oceanless, rotating Earth comprised of a mantle, fluid core and inner core. Surfaces of constant density are determined under the assumption of hydrostatic equilibrium between pressure and the combination of gravitational and centrifugal potential and are defined by the first two terms of eq. (4) in Section 3.1. Each region is allowed to deform elastically, but no dissipation effects are included. The reference equilibrium state is one of uniform rotation $\boldsymbol{\Omega}_{\rm o} = \Omega_{\rm o}\,\hat{\boldsymbol{e}}_{\boldsymbol{3}}$ with respect to a reference frame fixed to the mantle. The quantity of geophysical interest predicted by the model is the perturbation $\boldsymbol{\omega}$ which describes the changes in orientation of the Earth's rotation vector, or polar motion, with respect to the mantle.

The evolution of this polar motion is obtained by solving a system of four equations, the first three describing, respectively, the evolution of the angular momentum of the whole Earth ($\boldsymbol{H}$), the fluid core ($\boldsymbol{H_f}$) and the inner core ($\boldsymbol{H_s}$), and a fourth for the kinematic relation governing the tilt of the inner core relative to the mantle. For our present purpose, we replace the applied external torque by a torque on the inner core, and the four equations are

$$\frac{\mathrm{d}}{\mathrm{d}t}\boldsymbol{H} + \boldsymbol{\Omega}\times\boldsymbol{H} = \boldsymbol{0}, \tag{C1}$$

$$\frac{\mathrm{d}}{\mathrm{d}t}\boldsymbol{H_f} - \boldsymbol{\omega_f}\times\boldsymbol{H_f} = -\boldsymbol{\Gamma}_{\sigma}, \tag{C2}$$

$$\frac{\mathrm{d}}{\mathrm{d}t}\boldsymbol{H_s} + \boldsymbol{\Omega}\times\boldsymbol{H_s} = \boldsymbol{\Gamma_s} + \boldsymbol{\Gamma}_{\sigma} + \boldsymbol{\Gamma}_{V}, \tag{C3}$$

$$\frac{\mathrm{d}}{\mathrm{d}t}\boldsymbol{n_s} = \boldsymbol{\omega_s}\times\hat{\boldsymbol{e}}_{\boldsymbol{3}}. \tag{C4}$$

In these equations, $\boldsymbol{\Omega} = \boldsymbol{\Omega_o} + \boldsymbol{\omega}$ is the instantaneous rotation vector of the Earth, $\boldsymbol{\omega_f}$ and $\boldsymbol{\omega_s}$ are, respectively, the departures of the rotation axis of the fluid core and of the inner core with respect to $\boldsymbol{\Omega}$, and the tilt of the inner core $\boldsymbol{n_s} = \hat{\boldsymbol{e}}'_{\boldsymbol{3}} - \hat{\boldsymbol{e}}_{\boldsymbol{3}}$ is defined as the difference between the unit vectors $\hat{e}'_3$ and $\hat{e}_3$ pointing in the direction of the geometrical figure axis of, respectively, the inner core and the mantle. These are expressed in the conventional complex notation

$$\tilde{m} = m_1 + i m_2 = (\omega_1 + i\omega_2)/\,\Omega_{\rm o}, \tag{C5}$$

$$\tilde{m}_f = (m_f)_1 + i(m_f)_2 = [(\omega_f)_1 + i(\omega_f)_2]/\,\Omega_{\rm o}, \tag{C6}$$

$$\tilde{m}_s = (m_s)_1 + i(m_s)_2 = [(\omega_s)_1 + i(\omega_s)_2]/\,\Omega_{\rm o}, \tag{C7}$$

$$\tilde{n}_s = (n_s)_1 + i(n_s)_2, \tag{C8}$$

where the directions 1 and 2 refer to the two equatorial directions in the mantle reference frame.

The torque $\boldsymbol{\Gamma_s}$ represents the pressure and gravitational torques on a tilted inner core from the elliptical part of the density structure. In the forced nutation problem, the polar motion is that which results from a prescribed external torque from tidal forcing on the right-hand side of (C1). For our problem, no external torques participate, and the angular momentum of the whole Earth is conserved. We are interested instead in the polar motion resulting from internal torques on the inner core denoted by $\boldsymbol{\Gamma}_{\sigma}$ and $\boldsymbol{\Gamma}_{V}$. The torque $\boldsymbol{\Gamma}_{\sigma}$ is that produced by horizontal stresses at the ICB from non-hydrostatic fluid motions. This is the torque that was prescribed by Dumberry & Bloxham (2002). The torque $\boldsymbol{\Gamma}_{V}$ is the gravitational volume torque described in Section 3.3 and Appendix A.

Although the effect of $\boldsymbol{\Gamma}_{\sigma}$ on the polar motion is not the focus of the present study, we included it in the above system of equations to illustrate how its effect on the angular momentum dynamics is different than that of $\boldsymbol{\Gamma}_{V}$. Indeed, while both $\boldsymbol{\Gamma}_{\sigma}$ and $\boldsymbol{\Gamma}_{V}$ appear on the right-hand side of (C3), only $\boldsymbol{\Gamma}_{\sigma}$ is present on the right-hand side of (C2). The reason for the presence of $\boldsymbol{\Gamma}_{\sigma}$ in the fluid momentum equation is simple to interpret: as it is due to horizontal stresses on the surface of the inner core, the solid inner core necessarily produce the equal and opposite torque on the fluid core.

The reason why the same logic does not apply to $\boldsymbol{\Gamma}_{V}$ is explained by the argument that follows. In the absence of a torque from horizontal stresses at its solid boundary, the equation describing the angular momentum of the fluid core is (Sasao *et al.* 1980; Mathews *et al.* 1991a)

$$\frac{\mathrm{d}}{\mathrm{d}t}\boldsymbol{H_f} - \boldsymbol{\omega_f}\times\boldsymbol{H_f} = -\int_V \mathbf{r}\times(\boldsymbol{\nabla}P + \rho\boldsymbol{\nabla}\phi^f)\mathrm{d}V, \tag{C9}$$

where the integrated volume is the region occupied by the fluid core, P is pressure and ϕ^f the combined gravitational and centrifugal potential. At diurnal frequencies, the right-hand side plays a negligible role and can be eliminated from the fluid core's angular momentum balance (Sasao *et al.* 1980; Mathews *et al.* 1991a). This approximation remains valid for the decadal timescales of interests in our present study. In fact, at such timescales a simpler argument can be used: the fluid core remains in hydrostatic equilibrium even in its deformed state, and by definition $\boldsymbol{\nabla}P + \rho\boldsymbol{\nabla}\phi^f = 0$. The same reasoning can be used to explain the absence of $\boldsymbol{\Gamma}_{V}$ on the right-hand side of (C2). The deflection of equipotential contours in the fluid core produced by an inner core tilt is also accompanied by a coincident deflection of the density contours. The fluid core maintains its hydrostatic equilibrium which prevents the establishment of a volume torque acting on it. Therefore, there can be no $\boldsymbol{\Gamma}_{V}$ applied to the fluid core. The volume torque applied on the inner core does contain an influence from the fluid core, but only the part of the fluid core density which remains aligned with the mantle density anomalies; if the mantle were absent, no volume torque would ever develop between the inner and outer core. The hydrostatic deformations do lead to a small change in the moment of inertia of the fluid core, but these are included in $\boldsymbol{H_f}$.

We note that if one were to consider the volume gravitational torque on the solid Earth due to the density heterogeneities that drive convection in the core, the above reasoning does not apply. This is because these fluid motions are related to the non-hydrostatic part of the density. In this case, the torque from the solid Earth on the convective density heterogeneities in the fluid core must be included in the angular momentum balance. We neglect this latter torque in our study because the amplitude of the density anomalies that drive convection in the core are small (Stevenson 1987).

We note also that the torque $\boldsymbol{\Gamma_s}$ contains both a volume and surface component. Its surface component does not appear in (C2) only because it can be showed to be much smaller than the terms of the left-hand side of equation (Mathews *et al.* 1991a), and we omitted it here.

Proceeding with our adaptation of the nutation model, the system of eqs (C1)–(C4) is expanded as (Mathews *et al.* 1991a),

$$\mathbf{M}\cdot\boldsymbol{x} = \boldsymbol{b}, \tag{C10}$$

where $\boldsymbol{x} = [\tilde{m}, \tilde{m}_f, \tilde{m}_s, \tilde{n}_s]^T$ and $\boldsymbol{b}$ comprises the torques $\boldsymbol{\Gamma}_{V}$ and $\boldsymbol{\Gamma}_{\sigma}$. Among other quantities, the matrix $\mathbf{M}$ involves the equatorial

moments of inertia of the whole Earth (A), the mantle (A_m), the fluid core (A_f) and the inner core (A_s), the dynamical ellipticity (e), the elastic compliance (κ), and other parameters (α_1, α_3, α_g) whose exact definition can be found in Mathews *et al.* (1991a). All of these parameters can be calculated from a basic Earth model such as PREM (Dziewonski & Anderson 1981) and are given in Mathews *et al.* (1991b). (We note that the compliances given in Mathews *et al.* (1991b) are appropriate for diurnal timescales. At decade timescales, where inertial effects do not play a role in the balance of force that determines elastic deformations, some of these values may be different. However, because we do not require here the level of precision of the nutation study, these differences are inconsequential to the approximations that follow.)

The change in the moment of inertia that results from the axial rotation of the inner core, as determined in Appendix B, is incorporated by a redefinition of the deformation moments that enter the nutation equations. In the nutation formalism, the deformation moment of the whole Earth, written as $\tilde{c}_3$, is meant to capture the effect of elastic deformations caused by the rotation. We supplement this definition by adding the change in moment of inertia from $\tilde{c}_p$ as determined in (B5). Thus,

$$\tilde{c}_3 = A\left[\kappa\tilde{m} + \xi\tilde{m}_f + \zeta\tilde{m}_s\right] + \tilde{c}_p. \tag{C11}$$

where the first part contains the original definition of $\tilde{c}_3$ used in the nutation studies, with elastic compliances κ, ξ and ζ. We modify the deformation moments of the fluid core ($\tilde{c}_3^f$) and inner core ($\tilde{c}_3^s$) in a similar fashion, adding the contribution to the change in the moment of inertia of the fluid core $\tilde{c}_p^f$ and inner core $\tilde{c}_p^s$ induced by an inner core axial rotation.

We are interested in decade timescale dynamics, for which $d/dt \ll i\,\Omega_o$. In addition, the dynamical ellipticities and compliance factors are all $\mathcal{O}(10^{-3})$ or smaller. Eliminating small terms, we can express $\tilde{m}_s$ and $\tilde{m}_f$ as diagnostic equations in terms of $\tilde{m}$ and $\tilde{n}_s$: $\tilde{m}_s$ is obtained directly from (C4),

$$i\,\Omega_o\tilde{m}_s = -\frac{\mathrm{d}}{\mathrm{d}t}\tilde{n}_s, \tag{C12}$$

while $\tilde{m}_f$ is obtained from (C2)

$$i\,\Omega_o\tilde{m}_f = -\frac{\mathrm{d}}{\mathrm{d}t}\tilde{m} + \alpha_1 e_s\frac{A_s}{A_f}\frac{\mathrm{d}}{\mathrm{d}t}\tilde{n}_s - \frac{\tilde{\Gamma}_\sigma}{A_f\Omega_o}. \tag{C13}$$

In eq. (C13), the terms on the right-hand side represent, respectively, how the rotation vector of the fluid core is affected by the effect of a change in the rotation of the whole Earth, a change in its moment of inertia due to a tilted inner core, and surface torque acting at the ICB.

By inserting (C12) and (C13) into (C1) and (C3), and eliminating small terms, we get

$$\frac{\mathrm{d}}{\mathrm{d}t}\tilde{m} = a_{11}\tilde{m} + a_{12}\tilde{n}_s - \frac{\tilde{\Gamma}_V}{A_m\Omega_o} - \frac{i\,\Omega_o}{A_m}\tilde{c}_p, \tag{C14}$$

$$\frac{\mathrm{d}}{\mathrm{d}t}\tilde{n}_s = a_{21}\tilde{m} + a_{22}\tilde{n}_s - \frac{\tilde{\Gamma}_V + \tilde{\Gamma}_\sigma}{A_s\Omega_o} - \frac{\tilde{\Gamma}_V}{A_m\Omega_o} - \frac{i\,\Omega_o}{A_m}\tilde{c}_p, \tag{C15}$$

where

$$a_{11} = i\,\Omega_o\left[\frac{A}{A_m}(e-\kappa) - e_s\alpha_3\frac{A_s}{A_m}\right], \tag{C16}$$

$$a_{12} = i\,\Omega_o e_s\alpha_3\alpha_g\frac{A_s}{A_m}, \tag{C17}$$

$$a_{21} = i\,\Omega_o\left[\frac{A}{A_m}(e-\kappa) - e_s\alpha_3\left(1+\frac{A_s}{A_m}\right)\right], \tag{C18}$$

$$a_{22} = i\,\Omega_o e_s\alpha_3\left(1+\alpha_g+\alpha_g\frac{A_s}{A_m}\right), \tag{C19}$$

In writing (C14)–(C15), we have neglected terms that involve time-derivatives of $\tilde{c}_p$. The coupled equations (C14)–(C15) describe the evolution of the polar motion and inner core tilt as a function of imposed torques on the inner core from volume and surface forces, and as a function of the internal coupling that are triggered once the inner core is tilted with respect to the mantle and fluid core. The system of equations (C1)–(C4) contains four modes of free precession, while our reduced system (C14)–(C15) contains only two: the chandler wobble and the inner core wobble. Thus, one effect of the above approximations is to eliminate the two nearly diurnal free core nutations.

We note that subsequent to the manipulations above, eq. (C14) no longer represents the angular momentum balance for the whole Earth. Thus one should not be troubled by the appearance of an internal torque $\tilde{\Gamma}_V$. Rather, the coupled eqs (C14)–(C15) must be interpreted simply as representing the coupled evolution of the inner core tilt and the rotation vector of the whole Earth.